A

Dissertation on

A COMPARATIVE STUDY OF PERFORMANCE OF TCSC AND IMDU FOR DAMPING SSR IN SERIES COMPENSATED POWER SYSTEM

Submitted in partial fulfillment of the requirements for the award of degree of

Master of Technology

In

Power System

Under the supervision of:

Prof. Narendra Kumar

HOD

Electrical Department

Submitted by:

Prakash Chittora

MTech (Power System)

09/PS/2010

DEPARTMENT OF ELECTRICAL ENGINEERING

DELHI TECHNOLOGICAL UNIVERSITY

DELHI-110042

2010-2012

CERTIFICATE

This is to certify that the thesis entitled "**A Comparative study of Performance of TCSC and IMDU for damping SSR in series compensated Power System**" submitted by Prakash Chittora (09/PSY/2K10), in the partial fulfillment of the requirement for the award of degree of Master of Technology in Power System, Department of Electrical Engineering, Delhi Technological University, New Delhi, is an authentic work carried out by him under my supervision. To the best of my knowledge the matter embodied in the thesis has not been submitted to any other university/institute for the award of any degree or diploma.

Date:

(Prof. Narendra Kumar)
HOD
Department of Electrical Engineering,
Delhi Technological University,
New Delhi

ACKNOWLEDGEMENT

I feel honored in expressing my profound sense of gratitude and indebtedness to Prof. Narendra Kumar, Head of the Electrical Engineering Department, Delhi Technological University, Delhi for his guidance, meticulous efforts, constructive criticism, inspiring encouragement and invaluable co-operation which enabled me to enrich my knowledge and reproduce it in the present form.

I also like to extend my gratefulness to Sh. S.T. Nagarajan, Asst. Professor, for his perpetual encouragement, generous help and inspiring guidance.

I am also very thankful to the entire faculty and staff members of Electrical Engineering Department for their direct-indirect help, cooperation, love and affection, which made my stay at Delhi Technological University memorable,

I wish lo thank all my classmates for their time to time suggestions and cooperation without which I would not have been able to complete my work.

I would like to thank the Almighty, who has always guided me to work on the right path of the life, My greatest thanks are to my parents and brothers who bestowed ability and strength in me to complete this work.

Prakash Chittora
09/PS/2010

ABSTRACT

Series capacitive compensation has long been used as a means to increase the power transfer capability of a transmission line by reducing the inductive reactance of the line. This, however, may lead to sub-synchronous resonance (SSR).

An IMDU is a special high-power, low energy induction machine, with small rotor resistance and leakage reactance values, designed to operate close to synchronous speed. It is mechanically coupled to the turbo-generator (T-G) shaft and electrically connected to the generator bus.

The IEEE First Benchmark Models for subsynchronous studies is used to conduct eigenvalue analyses and time domain simulations. Time domain simulation studies were conducted with the IMDU in the mechanical system and TCSC along the network system. Simulations to study large transients were conducted. The coupling coefficient between IMDU and different turbine was fixed at the same value, and its effects on SSR mitigation and transient stability were observed. The best location providing maximum damping is next to the HP turbine at the end of the shaft.

This thesis present a simple design for TCSC scheme in which constant firing angle model is used. This thesis also shows that damping characteristics obtained by using IMDU are better than TCSC, But TCSC can be used for damping SSR as well as Controlling the active power flow.

The system results are obtained by modelling a linearized system in MALAB.

TABLE OF CONTENTS

LIST OF FIGURES

LIST OF TABLES

LIST OF SYMBOLS

AC	Alternating Current
C	Capacitor
v_a,v_b, v_c	Stator three-phase voltages, respectively
E_{fd}	Field voltage
EXC	Exciter
F	Frequency
GEN	Generator
HP	High pressure turbine
i_a, i_b, i_c	Stator currents in phase a, b, and c, respectively
IP	Intermediate pressure turbine
L	Inductor
LPA	Low pressure turbine A
LPB	Low pressure turbine B
P	Active power
p.u.	Per unit
Pe	Electrical power
Q	Reactive power
R	Resistor
RMS	Root mean square values
T_e	Air gap torque
Ψ_d , Ψ_q	Stator flux linkages in d-q components
δ_{GEN}	Generator power angle
X_C	Capacitive reactance
X_L	Inductive reactance
Δ	Prefix to denote a small deviation in the initial operating point

A	State matrix
B	Control or input matrix
C	Output matrix
D_{EXC}, D_{GEN}, D_{LPB}, D_{LPA}, D_{IP}, D_{HP} , D_{IM}	Damping coefficient of the corresponding inertia
S_{EXC}, S_{GEN}, S_{LPB}, S_{LPA}, S_{IP}, S_{HP} , S_{IM}	Slip of the corresponding inertia
IMDU	Induction machine damping unit
T_{GE}, T_{LBG}, T_{LAB}, T_{ILA}, T_{HI}, T_{PI}	Input torques to the respective Shaft section
O	suffix to denote the initial operating operation
ω_B	Natural frequency of system
σ^*	TCSC Conduction angle reference
TCSC	TCSC Controlled Series capacitor
C_{eff}	Effective TCSC Capacitance
X_{tl}	TCSC Inductance
X_{tc}	TCSC Capacitance
b_{Ceff}	Effective TCSC Susceptance
α	TCSC firing angle

Chapter 1
INTRODUCTION

1.1 Introduction

Growth of electric power transmission facilities is restricted despite the fact that bulk power transfers and use of transmission systems by third parties are increasing. Transmission bottlenecks, non-uniform utilization of facilities and unwanted parallel path or loop flows are not uncommon. Transmission system expansion is needed, but not easily accomplished. Factors that contribute to this situation include a variety of environmental, land-use and regulatory requirements. As a result, the utility industry is facing the challenge of the efficient utilization of the existing AC transmission lines.

FACTS controllers are power electronic based controllers which can influence transmission system voltage, currents, impedances and or phase angle rapidly. Thus, such controllers can improve the security of a power system by enhancing its steady state and transient stability or by damping the sub-synchronous resonance oscillations.

FACTS application studies require an understanding of the individual FACTS controllers as well as openness to the application of novel approaches.

Series capacitive compensation has long been used as a means to increase the power transfer capability of a transmission line by reducing the inductive reactance of the line. This, however, may lead to sub-synchronous resonance (SSR).

The natural frequency of resonance for a series compensated line is given by [1]

$$f_{resonance} = \frac{1}{2\Pi\sqrt{L_{system}C_{line}}} \qquad \text{Eq. 1.1}$$

Damping SSR oscillations has been a topic of great interest and research. Early strategies suggested dissipating the energy during resonance in resistor banks [2]. Countermeasures utilizing TCSC, NGH schemes [3]–[5], phase shifters [6], excitation controllers, and static VAR compensators [7] have been extensively researched through the years. Numerous modeling techniques and improvements on these schemes have also been given [8], [9]. The use of stored magnetic energy has been published in [10]–[12].

The concept of the induction machine damping unit (IMDU) as a countermeasure to SSR was devised in [13] and extended in [14]. These papers stated the possibility of damping SSR using an IMDU in conjunction with additional control for static VAR systems.

A system similar to the IEEE First Benchmark Model (FBM) [16] was utilized in these papers, while assuming negligible mass for the IMDU. In this paper, we use an IMDU to Eliminate SSR.

An IMDU is a special high-power, low energy induction machine, with small rotor resistance and leakage reactance values, designed to operate close to synchronous speed. It is mechanically coupled to the turbo-generator (T-G) shaft and electrically connected to the generator bus.

The main contributions of this report include:

1. Putting forward the possibility of damping SSR with only an IMDU (no controllers needed) coupled to the shaft of the T-G, and corresponding IMDU parameters.
2. Putting forward the possibility of damping SSR with TCSC with suitable controller and TCSC parameters.
3. Comparative study of both TCSC and IMDU methods of damping Sub-Synchronous resonance.

The IEEE First Benchmark Models for subsynchronous studies is used to conduct eigenvalue analyses and time domain simulations. Time domain simulation studies were conducted with the IMDU at the shaft HP end and with TCSC connected to network. Simulations to study large transients were conducted.

Studies were carried out on both devices to find the best location so that SSR is effectively mitigated.

1.2 Induction Machine Damping Unit (IMDU)

The problem of torsional oscillations occurs because of active power imbalance (a difference between turbine input and generator output) during rotor swing, but only few work has been reported for handling this problem through active power control.

The damping unit is an induction machine running at synchronous speed during steady state, consequently consuming or generating no power. In fact, it can even be electrically disconnected, drawing no magnetizing current.

The property of an induction machine to act either as a generator or motor is utilized to absorb mechanical power if there is excess and to release it when there is a deficiency.

High pressure (HP) and other turbines produce torque in the direction of rotation (forward direction) and the generator produces the electromagnetic torque in the opposite direction.

The T-G set has a long shaft and consequently the turbine and generator torques produce an angular twist in the shaft. The twist angle is dependent on load, and during steady-state operation it is constant. However, during the torsional oscillating state the angle varies periodically. If the system has negative damping, the amplitude of the torsional oscillations will grow exponentially which may damage the shaft.

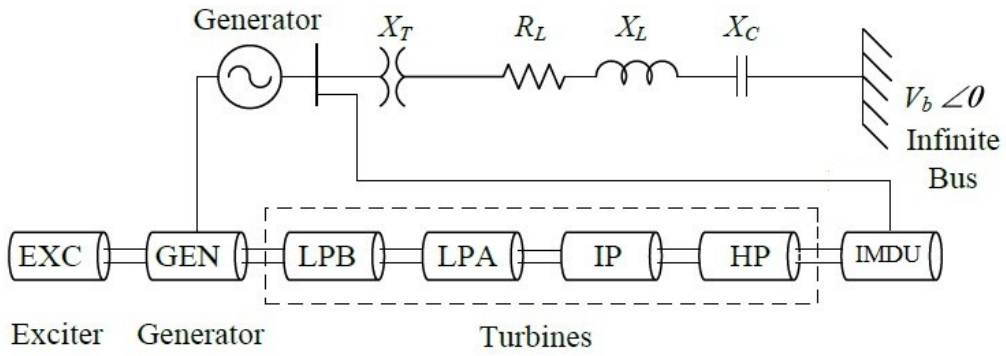

Figure 1.1 IMDU Connected to the System

If an induction machine is connected to the HP turbine on its right side as shown in Fig. 1.1 and if the speed of the machine exceeds the synchronous speed (mechanical input is greater than electrical output of generator) the machine acts as an induction generator. Torque produced by it is in the reverse direction. It can be visualized that this torque will tend to reduce the twist angle (δ), hence it reduces the amplitude of torsional oscillation. Alternatively, it can be said that it increases the damping of the system.

If the speed of the shaft is less than the synchronous speed, the induction machine will act as a motor and it produces a torque in the forward direction. In this operation, it supports the turbine torque and helps to restore the speed.

So in any case it tries to oppose the change in the synchronous speed of the shaft. It can be said that it reduces the oscillations in the rotating mass around the nominal speed, or that the damping of the system is increased.

Since this machine comes into operation during transients only, it is designed for very high short-term rating and very small continuous rating; consequently the machine has low inertia, low power, small size and low cost.

Because of its small mass and tight coupling with the high pressure turbine it has been considered a single mass unit with the HP turbine. Electrically it is connected to the generator bus.

1.3 FACTS: Flexible AC Transmission System

FACTS devices that have an integrated control function are known as FACTS Controllers. FACTS controllers are high-voltage, high-current solid-state controllers[25] capable of controlling the interrelated line parameters and other operating variables that govern the operation of transmission systems including series impedance, shunt impedance, current, voltage, phase angle and damping of oscillations at various frequencies below the rated frequency [25-27]. There are many types of FACTS devices that are in use today:

1. Thyristor-Switched Capacitor (TSC),
2. Thyristor-Controlled Reactor (TCR),
3. Static VAR Compensator (SVC),
4. Static Synchronous Compensator(STATCOM),
5. Thyristor-Switched Series Capacitor (TSSC),
6. Thyristor-Controlled Series Capacitor (TCSC),
7. Static Series Synchronous Compensator (SSSC),
8. Unified Power Flow Compensator (UPFC),
9. Interline Power Flow Compensator (IPFC) .

1.3.1 Thyristor-Switched Capacitor

A thyristor-switched capacitor (TSC) consists of a fixed capacitor C, a bidirectional thyristor switch SW, and a relatively small surge-limiting reactor L as shown in Figure 1.2. The switch is used to either insert or remove the capacitor from the electric network. The steady state current through the capacitor for a transient-free operation is given as [25]:

$$i(t) = v_m \frac{n^2}{n^2 - 1} \omega c \cos(\omega t + 90) = -v_m \frac{n^2}{n^2 - 1} \omega c \sin(\omega t)$$

Eq. 1.2

Where Vm is the maximum peak voltage across the TSC, $n = \sqrt{X_C / X_L}$ is the system angular speed and C is the capacitance of the shunt capacitor.

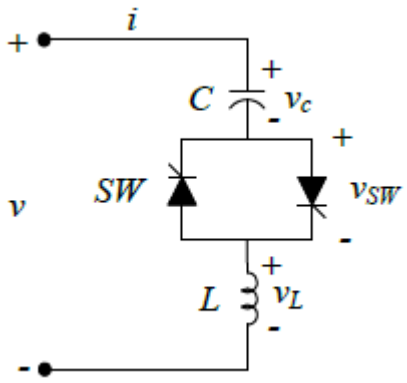

Figure 1.2 Thyristor-Switched Capacitor

The TSC can be disconnected at zero current by prior removal of the thyristor-gating signal. It gives variable shunt capacitor compensation by chopping the amount of current (i.e. by varying the thyristor firing angle) passing through it.

1.3.2 Thyristor-Controlled Reactor

A thyristor-controlled reactor (TCR) consists of a fixed reactor of inductance L and a bidirectional thyristor switch SW, as shown in Figure 1.3. The current through the reactor can be controlled from zero to a maximum by varying the delay angle, of the thyristor firing. The fundamental root-mean-square (RMS) component of the current passing through the reactor can be expressed in terms of the thyristor firing angle α, as [25]:

$$i_L(\alpha) = \frac{V}{\omega L}(1 - \frac{2}{\pi}\alpha - \frac{1}{\pi}\sin 2\alpha) \qquad \text{Eq. 1.3}$$

and the admittance as a function of α is given as:

$$Y_L(\alpha) = \frac{I_L}{V} = \frac{1}{\omega L}(1 - \frac{2}{\pi}\alpha - \frac{1}{\pi}\sin 2\alpha) \qquad \text{Eq. 1.4}$$

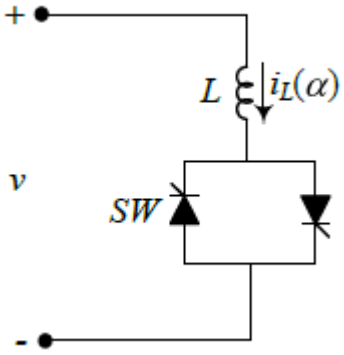

Figure 1.3 Thyristor-Controlled Reactor (TCR)

where V is the RMS value of the system voltage ,ω is the system angular speed, and L is the inductance of the shunt inductor. The admittance $Y_L(\alpha)$ can be varied by varying the thyristor firing angle α, and hence the inductive compensating current.

1.3.3 Static VAR Compensator

The use of either TCR or TSC would allow only variable inductive or capacitive compensation. However, in most applications, it is desirable to use both capacitive and inductive compensations. A static VAR compensator (SVC) consists of TCRs in parallel with one or more TSCs. A schematic diagram of SVC is shown in Figure 1.4. The reactive elements are connected to the high voltage system through a step-down transformer. The controller is used to switch *on* and *off* the capacitor and inductor banks thyristor gates at exact pre-calculated timing.

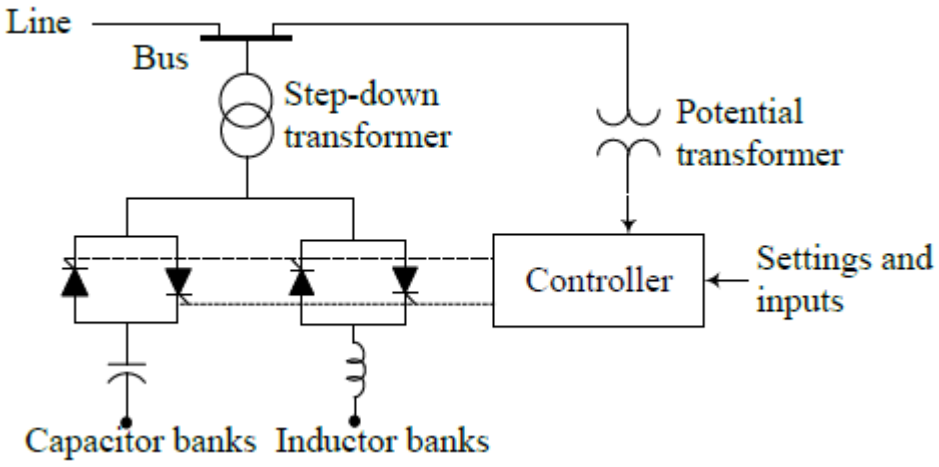

Figure 1.4 Static VAR Compensator schematic diagram.

1.3.4 Static Synchronous Compensator

A Static Synchronous Compensator (STATCOM) is also known as an advanced static VAR compensator. It is capable of generating or absorbing independently controllable real and reactive power at its output terminals when it is fed from an energy source or energy-storage device at its input terminals. The functionality of a STATCOM can be understood with the help of a traditional synchronous condenser. Figure 1.5 shows a synchronous condenser schematic diagram.

For a purely reactive power flow, the three-phase induced electromotive forces ,e_a ,e_b ,e_c of the synchronous rotating machine are in phase with the system voltages , v_a v_b v_c . The reactive current drawn by synchronous compensator is determined by the magnitude of

the system voltage *Vpcc*, and the internal voltage E_g. The reactive current and reactive power expressions are given as:

$$I = \frac{V_{pcc} - E_g}{X_T} \qquad \text{Eq. 1.5}$$

$$Q = \frac{1 - E_g / V_{pcc}}{X_T} V_{pcc}^{\ 2} \qquad \text{Eq. 1.6}$$

Where X_T is the sum of transformer leakage reactance, synchronous machine reactance, and system short-circuit reactance.

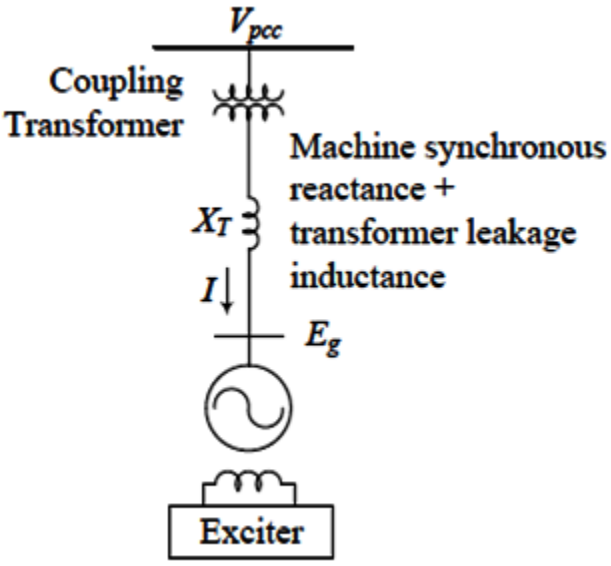

Figure 1.5 Static Synchronous Compensator

1.3.5 Thyristor-Switched Series Capacitor

A thyristor-switched series capacitor (TSSC) consists of a number of capacitors in series, each shunted by a switch composed of two anti-parallel thyristors as shown in Figure 1.6. A capacitor is inserted in the transmission line by turning '*off*' the thyristors, and it is bypassed by turning '*on*' the thyristor switch. The equivalent capacitance, for $C_1 = C_2 \ldots = C_1$ is:

C_{eq}= C/m if m Thyristor switches are switched *'off'*

C_{eq}= 0 if all the Thyristor switches are switched *'on*

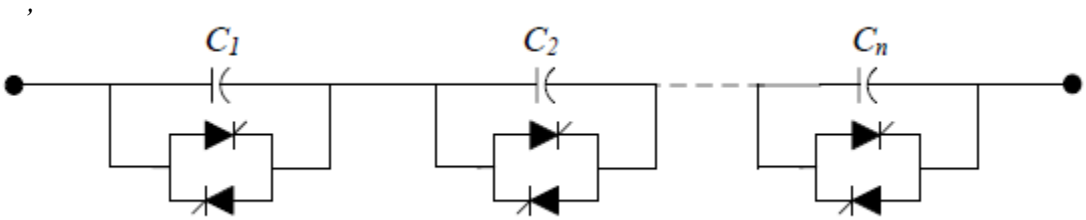

Figure 1.6 Thyristor-switched series capacitor schematic diagram

1.3.6 Thyristor-Controlled Series Capacitor

Thyristor-controlled series capacitor (TCSC) [28] consists of a series capacitor shunted by a thyristor-controlled reactor. A schematic diagram of the TCSC is shown in Figure 1.7. In practical implementations, several such compensators are connected in series to obtain the desired voltage rating and operating characteristics.

The basic purpose of the TCSC scheme is to provide continuously variable capacitor compensation by means of partially canceling the effective compensating capacitance by the TCR.

The effective reactance obtained using this configuration is [25]:

$$X_{TCSC}(\alpha) = \frac{X_C X_L(\alpha)}{X_L(\alpha) - X_C} \qquad \text{Eq. 1.7}$$

Where X_C is capacitive reactance of capacitor, $X_L = \omega L$ and value of $X_L(\alpha)$ is derived from Eq. (1.4) as:

$$X_L(\alpha) = \frac{1}{Y_L(\alpha)} = X_L \frac{\pi}{\pi - 2\alpha - \sin 2\alpha}; X_L \le X_L(\alpha) \le \infty \qquad \text{Eq. 1.8}$$

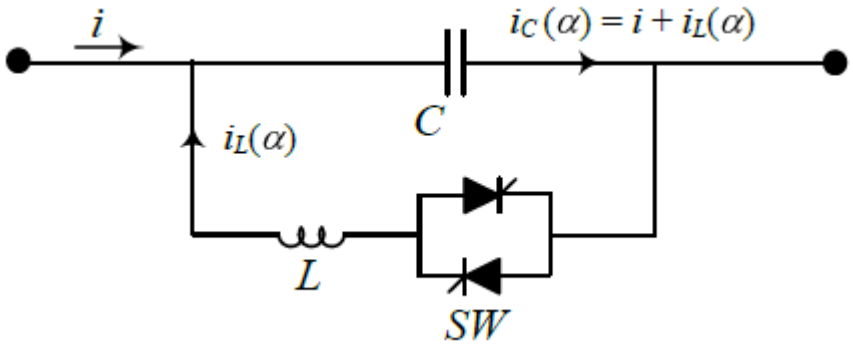

Figure 1.7 Thyristor-controlled series capacitor

By varying the thyristor firing angle α, the effective series compensating reactance can be varied. If the impedance of X_L is sufficiently smaller than X_C, the '*on*' and '*off*' operation of the TCSC can be controlled in the same way as a TSSC. For the usual TCSC arrangement in which the impedance of the TCR reactor X_L, is smaller than that of the capacitor X_C, the TCSC has two operating ranges around its internal circuit resonance [25]:

i. $X_{TCSC}(\alpha)$ is capacitive when $\alpha_{clim} \leq \alpha \leq \pi/2$, where α_{clim} is minimum value of α in capacitive region to avoid resonance.

ii. $X_{TCSC}(\alpha)$ is inductive when $0 \leq \alpha \leq \alpha_{Llim}$, where α_{Llim} is maximum value of α in inductive region to avoid resonance.

1.3.7 Static Synchronous Series Compensator

The Static Synchronous Series Compensator (SSSC) uses a power electronic based voltage-source converter with a capacitor or capacitors in its dc side to replace the switched capacitors in the conventional series compensator. The converter output is arranged to appear in series with the transmission line via the use of a series transformer. The converter output voltage $\boldsymbol{V_{inj}}$, which can be set to any relative phase, and any magnitude within its operational limits, is adjusted to appear to lead the line current by 90^o, thus behaving as a capacitor.

This type of series compensation can provide a wide range of series compensation by varying the magnitude of $\boldsymbol{V_{inj}}$. Further, it can reverse the phase of $\boldsymbol{V_{inj}}$, thereby increasing the overall line reactance; this may be desirable to limit fault current, or to dampen power system oscillations.

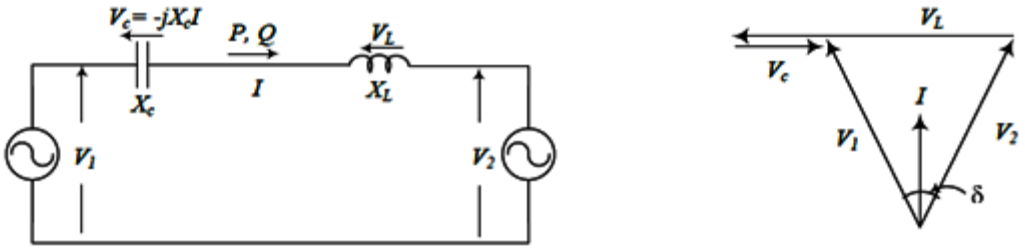

Figure 1.8 A basic two machine system with a series capacitor compensated line and associated phasor diagram.

$$V_{inj} = V_C = -jX_C I = -jkX_L I \qquad \text{Eq. 1.9}$$

Where,

V_C = Voltage across capacitor,

I = Line current,

X_L = Transmission line reactance,

k = Degree of series compensation ($k=X_C/X_L$).

By making the output voltage of the static synchronous voltage-source a function of the line current as shown in Eq. (1.9), the same compensation provided by the series capacitor can be accomplished. However, in contrast to the real series capacitor, the static voltage-source is able to maintain a constant compensating voltage in the presence of a variable line current, or control the amplitude of the injected compensating voltage independent of the amplitude of the line current.

1.3.8 Unified Power Flow Controller

A unified power flow controller (UPFC) consists of a STATCOM and a SSSC connected to the common dc link as shown in Figure 1.9. The real power drawn or generated by the shunt compensator is always equal to the real power generated or drawn by the series compensator. The reactive power in the shunt or series converter can be independently controlled at a desired level, thus, enabling greater flexibility to the power flow control. The UPFC can be used to control, simultaneously or selectively, all the parameters affecting power flow in the transmission line (i.e., voltage, impedance, and phase angle) [25].

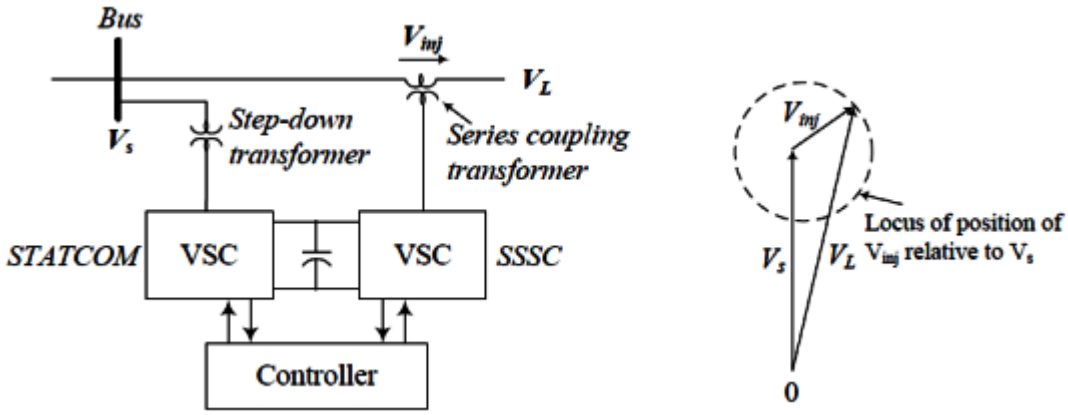

Figure 1.9 Unified Power Flow Controller and associated phasor diagram.

1.3.9 Interline Power Flow Controller

The interline power flow controller (IPFC) implements a number of independently controllable series reactive compensators in individual parallel transmission lines to provide a capability to directly transfer real power between the compensated lines. This capability makes it possible to equalize both real and reactive power flow between lines. Following are some advantages of the IPFC.

- **i.** Reduces the burden of overloaded lines by real power transfer.
- **ii.** Compensates against resistive line voltage drops and the corresponding reactive power demand.
- **iii.** Increases the effectiveness of the overall compensating system for dynamic disturbances.

The schematic diagram with IPFC placed on n sets of parallel transmission lines is shown in Figure 1.10.

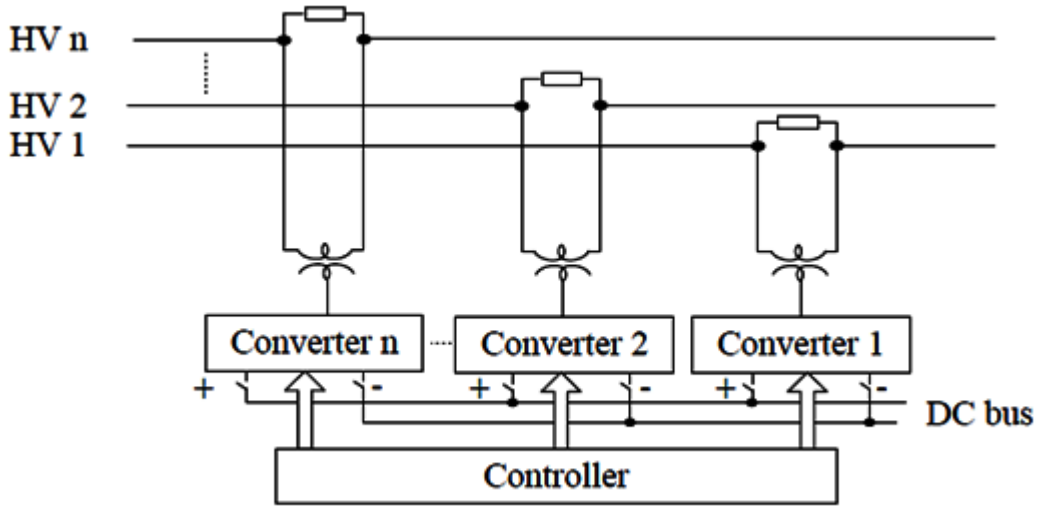

Figure 1.10 Interline Power Flow Controller schematic diagram

1.4 Subsynchronous Resonance: Basic Phenomenon

Subsynchronous resonance is a phenomenon associated with the energy exchanged between the turbine-generator mechanical and electrical systems. A number of mechanical masses of the turbine-generator shaft (e.g. turbine stages and generator) oscillate at some frequencies known as torsional oscillations which are characterized by their mechanical properties like spring constants and mass inertia. The frequencies of these oscillations range from 10 to 55 Hz for 60 Hz system [17].

The oscillation of the generator rotor at a subsynchronous frequency 'f_m' results in voltages induced in the armature having components of:

(i) Sub-synchronous frequency ($f_0 - f_m$).

(ii) Super-synchronous frequency ($f_0 + f_m$).

Where 'f_0' is the operating frequency. These voltages setup currents in the armature (and network), whose magnitudes and phase angles depend on the network impedances. The super-synchronous frequency currents result in positive damping torque while the sub-synchronous frequency results in negative damping torque [18]. If the series capacitive compensated electrical network has a torsional frequency around ($f_0 - f_m$), the torsional oscillation will amplify, resulting in a shaft fatigue or damage.

This kind of interaction between the series capacitor and the turbine-generator shaft system is known as "Sub-synchronous Resonance" or "SSR" [1].

1.4.1 Definition

The IEEE definition of subsynchronous oscillation is [1]:

"Subsynchronous oscillation is an electric power system condition where the electric network exchanges significant energy with a turbine-generator at one or more of the natural frequencies of the combined system below the synchronous frequency of the system following a disturbance from equilibrium".

Electrical power generation involves interaction between the electrical and mechanical energies coupled through the generator. It follows that any change in the electric power system results in a corresponding reaction/response from the mechanical system and vice versa. Slow-changing load translates to a slow-changing mechanical torque on the rotor shaft, which in turn, is matched by a slow-changing rotor angle to new steady-state angle between the rotor and the stator along with adjustment in the mechanical power input to the rotor through the turbines. Major disturbances such as faults and fault clearing result in large transient torques on the mechanical system and corresponding transient twisting of the rotor shaft couplings between tandem turbines and generator .

A typical rotor of a large turbine-generator consists of several rotating masses; turbine stages, a generator, and often a rotor of a rotating exciter as shown in Figure 1.11. The rotor masses and coupling shafts form a spring-mass system which has intrinsic modes of torsional natural frequencies which are always below the synchronous frequency [19]. There are generally modes of torsional oscillations for an *m*-mass-spring system, in addition to a zero mode by which the entire mass-spring system oscillates as a rigid body. The mechanical damping for the torsional vibration is always low but positive, which is mainly due to friction,

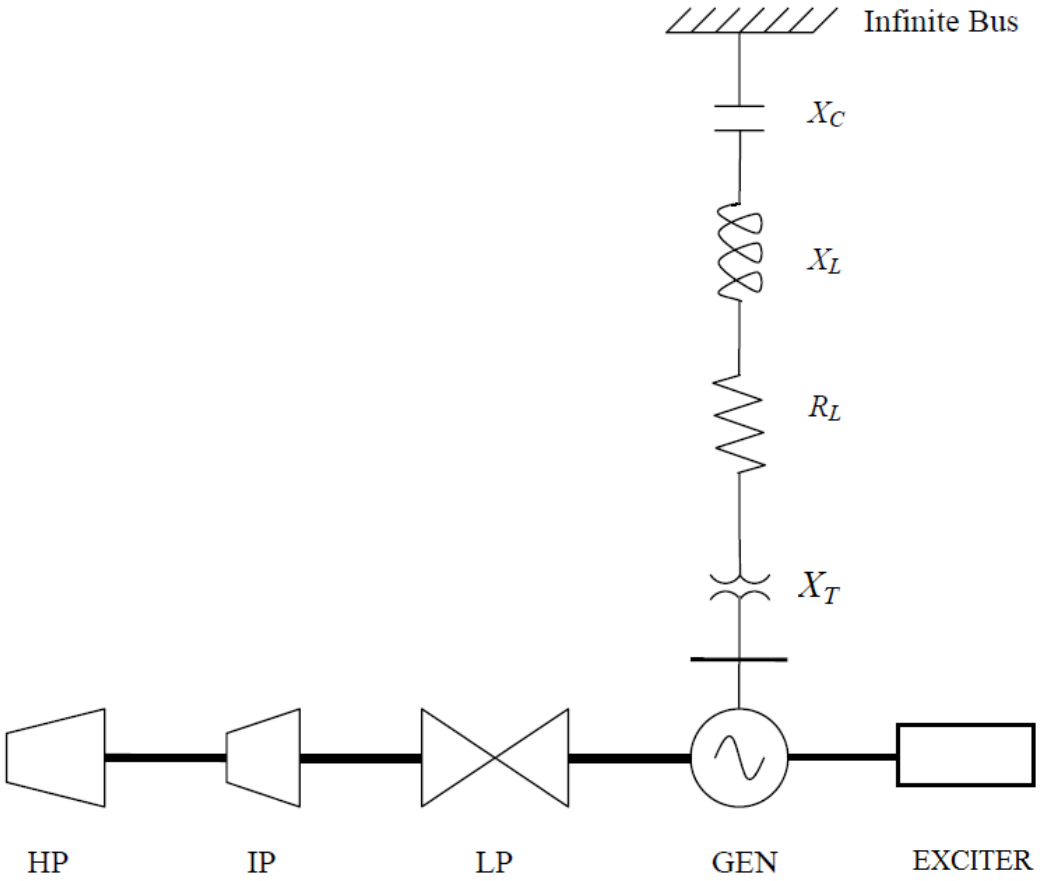

Figure 1.11 A schematic diagram of a series compensated single machine infinite bus system.

A single machine infinite bus system with the series capacitor compensated transmission line shown above in Figure 1.11 will have a resonance frequency f_e given by [18]:

$$f_e = f_0\sqrt{\frac{X_C}{X''+X_L+X_T}} = f_0\sqrt{\frac{X_C}{X_{tot}}} \qquad \text{Eq. 1.10}$$

where, 'f_0' is system nominal frequency, X'' is sub-transient reactance of the generator, X_T is transformer leakage reactance, X_L is transmission line inductive reactance, R_L is total transmission line resistance, and X_C is the capacitive reactance. The compensation level k = X_C / X_L is always less than unity as $X_C < X_L$. It is more likely that the electrical resonant frequency is close to one of the compliments of torsional oscillation frequency (i.e. f_0 - f_m) exciting the torsional mode of oscillation. In such a condition, the electrical damping of the system becomes negative and sub-synchronous oscillations can build up from a very small disturbance. To avoid this problem, the series compensation level can

be selected such that its value does not lie near one of the compliments of torsional oscillation frequency. However, this is very difficult to achieve as the value of X_{tot} depends on the continuous changing system configuration due to planned and unplanned line switching.

1.4.2 Impact of Phase Imbalance on SSR

The coupling between the electrical and mechanical sides in a synchronous generator occurs through an interaction between the driving mechanical torque and a developed electromagnetic torque. The electromagnetic torque is developed by the interaction of the machine currents with the magnetic fields, namely the interaction of the armature currents with the rotor magnetic field and the interaction of the rotor currents with the armature magnetic field. The three-phase currents in the armature windings have their full capability of developing interacting electromagnetic torque when they are balanced in the time and space domains. In this balanced condition, the three-phase currents create a circular rotating magnetic field of a constant amplitude and speed. Unbalanced currents [20], on the other hand, create an elliptical rotating field which has a time varying amplitude and speed. The elliptical field, however, is equivalent to a circular rotating field component, and a pulsating field component, of comparatively lower magnitude. This means that phase imbalance weakens the electromechanical coupling, and as a result, reduces the energy exchange between the turbine-generator electrical and mechanical sides.

1.4.3 Types of SSR Interactions

There are two types of SSR interactions [18]:

1.4.3.1. Self excitation or steady state SSR

The subsynchronous frequency current entering the generator terminals produces subsynchronous frequency terminal voltage components. These voltage components may sustain the currents to produce self excitation. There are two types of self excitation:

1.4.3.1.1. Induction generator effect

The electrical resonance due to the series capacitor compensated transmission line creates a revolving field on the generator stator corresponding to the resonant frequency. For the highly compensated transmission line, the electrical resonance frequency f_e ,will be less than system nominal frequency f_0, and the resonant current drawn by the electrical network causes a rotating field at subsynchronous frequency. Since the generator rotor is rotating at

synchronous frequency, the synchronous machine behaves like an induction generator with respect to the subsynchronously rotating field. The slip of the machine viewed as an induction generator is given by the relation:

$$s = (f_e - f_0)/f_e < 0, \quad \text{For } f_e < f_0 \qquad \text{Eq. 1.11}$$

As the slip is negative, the equivalent resistance viewed from the armature terminals is negative and when this magnitude of the negative resistance exceeds the sum of the armature and network resistance at a resonant frequency, there will be a self excitation.

1.4.3.1.2. Torsional Interaction

The generator rotor torsional oscillation frequency f_m, induces armature voltage components at the frequencies given by:

$$f_{em} = f_0 \pm f_m \qquad \text{Eq. 1.12}$$

When the sub-synchronous frequency component of f_{em} coincides or is very close to an electric resonance frequency f_e " of the generator and transmission system, the torsional oscillation and electrical resonance will be mutually excited resulting in SSR. In such a case, the electrical resonance acts as a negative damping to the torsional oscillation, and the torsional oscillation acts as a negative resistance to the electrical resonance.

1.4.3.2. Transient Torques or Transient SSR

Transient torques are those that result from system disturbances. System disturbances cause sudden changes in the network, resulting in sudden changes in the currents that will tend to oscillate at the natural frequencies of the network. In a transmission system without series capacitors, these transients decay to zero with a time constant that depends on the ratio of inductance to resistance. For the series capacitor compensated transmission line, the transient torque contains many components including unidirectional, exponentially decaying and oscillatory torques from subsynchronous to multiples (typically second harmonic) of the network frequency. Due to the SSR phenomenon, the subsynchronous frequency component of torque can have a large amplitude immediately following large disturbances, although it may decay eventually [18]. Such large amplitude subsynchronous torque degrades the shaft life and is cumulative in nature.

1.4.4 SSR Analysis Tools

The SSR phenomenon involves energy exchange between mechanical and electrical systems. Therefore, the detailed representation of both electromechanical dynamics of the generating units and the electromagnetic dynamics of the transmission network is required for the analysis of SSR. There are several methods available for the study of SSR and some commonly used methods are described in brief in this section.

1.4.4.1. Frequency Scanning

This technique computes the equivalent resistance and inductance seen from the stator winding of the generator to the network as a function of frequency. If there is a frequency at which the inductance is zero and the resistance is negative, self sustaining oscillations would be expected due to the induction generator effect. This method is particularly suited for preliminary analysis of SSR problems.

1.4.4.2. Eigenvalue Analysis

This is performed with the network and the generator modeled by a system of linear simultaneous differential equations. The results provide both the natural frequencies of oscillation as well as the damping of each frequency.

This technique, thus, will be used for conducting the small-signal analysis to provide a comprehensive understanding of the various aspects of the SSR phenomenon.

The performance of a dynamic system, such as the power system, may be described by a set of *n* first-order nonlinear ordinary differential equations, which may be linearized in the following standard expression:

$$\Delta \dot{X} = A\Delta X + B\Delta U \qquad \text{Eq. 1.13}$$

Where,

Δ --- prefix to denote a small deviation about the initial operating point

ΔX --- the state vector

ΔU --- the input vector

A --- the state matrix

B --- the control or input matrix

The stability of the system is given by the eigenvalues of matrix A as follows:

1. A real eigenvalue is associated with a non-oscillatory mode. A negative real

eigenvalue represents a decaying mode. The larger its absolute value, the fast is the decay. A positive real eigenvalue represents aperiodic instability.

2. Complex eigenvalues always occur as conjugate pairs, and each pair corresponds to an oscillatory mode. The real part of the eigenvalues represents the damping, and the imaginary part represents the frequency of oscillation. A negative real component represents a damped oscillation; on the other hand, a positive real component represents an oscillation with an increasing amplitude.

Therefore, the negativeness of the real part of all eigenvalues assures the system stability. The more negative the real part, the sooner the response of the associated mode dies.

Chapter 2
Literature Review

2.1 Introduction

Series capacitors have been extensively used as a very effective means of increasing power transfer capability of transmission system, and improving transient and steady state stability limits of a power system. This is due to partially compensating the reactance of the transmission lines. The dynamic behavior of power system is quite complex and a good understanding is essential for proper system planning and secure operation.

Subsynchronous resonance (SSR) in series compensated power system is a phenomenon implying an undesirable energy exchange between electrical and mechanical sides of turbine generator sets at a frequency below resonant frequency .

Since the discovery in 1970 that SSR was the main cause of shaft failure at Mohave power plant [17] in Southern Naveda, extensive research and development of effective SSR mitigating measures [2-16]. Among these IMDU has gained importance in recent years.

The chapters in this thesis presents a comprehensive review about the device used for damping Subsynchronous phenomenon (SSR) by using IMDU and TCSC. TCSC is used as a series device and IMDU is connected to mechanical system of system.

O. Wasynczuk [2], shows the technical feasibility of using a dynamically controlled; three phase resistor bank to damp shaft torsional oscillations in large steam turbo-generators. Torsional damping was achieved using a straightforward control strategy based on generator speed. It was shown that substantial damping can be achieved with a relatively small resistor bank, thus reducing the risk of significant shaft damage due to electrical disturbances.

E. Gustafson, A. Aberg, and K. J. Astrom [3], proposed a method which uses only measurements available at the series capacitor located anywhere at the transmission line. The generator rotor position and angular velocity were estimated and a thyristor controlled series capacitor (TCSC) was used to create an active damping torque that rapidly damps all subsynchronous oscillations of the turbine-generator system.

N. Kakimoto and A. Phongphanphanee [4] proposed that With an appropriate angle of thyristor firing, electrical damping becomes almost zero, which is called SSR neutral.

This quality comes from TCSC itself. However, negative damping still remains and is large for firing angle 170-800° where little current flows through thyristors. This paper deals with control of firing angle. First, we oscillate the firing angle at a given frequency, Next, it was shown that the damping improves at all frequencies if the firing angle oscillation is in phase with that of rotor angle.

H. Sugimoto, M. Goto, W. Kai, Y. Yokomizu, and T. Matsumura [5], described comparative studies among the power electronics devices that can suppress the SSR. Computer simulations were made to evaluate the SSR damping effect, the loss in the resistor and the necessary thyristor rated capacity for three different countermeasures (Narain G. Hingorani scheme (NGH), thyristor controlled series capacitor (TCSC) and dynamic stabiliser (DS)) to SSR. The results of this study show that the DS scheme can decrease the cost of equipment more than the other schemes because of the lowest thyristor rated capacity. However, the damping effect of SSR in case of applying DS scheme was the weakest among all ofthe schemes.

M. R. Iravani and R. M. Mathur [6], proposed a method which utilized a thyristor-controlled phase-shifter to modulate the generator active power by injecting a quadrature phase voltage in the system. The rotor speed deviation from the synchronous speed was used as the control signal. An eigenvalue analysis and the complex torque coefficient methods were used to demonstrate the technical feasibility of a static phase-shifter for damping SSR. The analytical results are verified by a detailed digital computer study on the first IEEE benchmark for SSR studies.

L.Wang and Y. Y. Hsu [7], show comparative study on the application of two countermeasures, i.e. the excitation controller and the static VAr compensator (SVC), for damping of subsynchronous resonance (SSR). The two damping schemes differ in the way they modulate the reactive power flow in the system to damp out the subsynchronous oscillations. The relative merits of the two countermeasures were compared with respect to their validities under various loading conditions and different degrees of series compensations and their capabilities to expand the stable region on the real-capacitive reactance plane.

B. K. Perkins and M. R. Iravani [8], proposed dynamic modeling of TCSC to damp SSR.

X. Zhao and C. Chen [9], put forward an improved NGH SSR damping scheme and presented digital simulation results of the same on damping unstable torsional oscillations that occur in the IEEE First Benchmark Model, which contain a turbine-generator set connected to an infinite bus through a series compensated transmission line.

The improved NGH scheme adds SSR detection and prefiring functions on the basis of the original NGH scheme invented by Narain G. Hingorani. The basic principle of the improved scheme was described as well as the fundamental concepts of the original scheme.

W. Li, L. Shin-Muh, and H. Ching-Lien [10], proposed a novel damping scheme using superconducting magnetic energy storage (SMES) unit to damp subsynchronous resonance (SSR) of the IEEE Second Benchmark Model, system-1 which is a widely employed standard model for computer simulation of power system SSR. The studied system contains a turbine-generator set connected to an infinite bus through two parallel transmission lines, one of which is series-capacitor compensated. In order to stabilize all SSR modes, simultaneous active and reactive power modulation and a proportional-integral-derivative (PID) damping controller designed by modal control theory were proposed for the SMES unit. A frequency domain approach based on eigenvalue analysis and time-domain approach based on nonlinear model simulations were performed to validate the effectiveness of the damping method.

A. H. M. A. Rahim, A. M. Mohammad, and M. R. Khan [11], also extend the concept of damping SSR with the help of superconducting magnetic energy storage units.

O. Wasynczuk [12], investigate a method of damping SSR which utilizes a small AC-DC converter connected to the machine bus of the affected generator. The DC side of the converter connects to a large inductor which was used to store energy. Various methods of controlling this inductor converter unit were proposed and analyzed. The effectiveness of these control methods was demonstrated by a detailed computer simulation of a benchmark system known to be affected by subsynchronous resonance.

S. K. Gupta, A. K. Gupta, and N. Kumar [13], first introduces Damping SSR by an Induction machine damping unit. IMDU is a versatile device which can act as both as a motor and generator so that it can absorb SSR oscillations very well. Detailed analysis were conducted to damping properties of IMDU and it was shown that IMDU has good ability to handle SSR at all level of power transfer conditions.

K. Narendra [14], further develop IMDU model for SSR studies.

S. Purushothaman [15], extend to Second Benchmark Models for subsynchronous resonance (SSR) to analyze the damping properties of an induction machine damping unit (IMDU) coupled to the shaft of a turbo-generator set. This paper investigates the rating and location of the induction machine that, without the aid of any controllers, effectively damps subsynchronous resonance for all line series compensation levels.

Eigenvalue analyses were performed on linearized models of the shaft system including the induction machine to find the optimum location. The best location of the IMDU, providing maximum damping, was next to the HP turbine at the end of the shaft. It was observed that a small size, high power (about 10% of the generator rating), low energy machine effectively damps SSR. The IMDU reduces peak torques in shaft sections during transients. In the paper, it was demonstrated that the addition of an IMDU at the end of the shaft would have prevented the SSR events of the Mohave Desert shafts.

G.N. Pillani, Arindam Ghosh and A. Joshi [19] demonstrated the application of SSSC in combination with fixed capacitor to avoid torsional mode instability.

A. A. Edris [20], proposed phase imbalance techniques for SSR studies.

Paolo Mattavelli, Alexander M Stankovic and George C Verghese [24] paper presented the use of a dynamic phasor model of the TCSC in studies of subsynchronous resonance (SSR). The proposed approach to SSR analysis was an attractive alternative to approaches based on sampled-data models, and to torque-per-unit-velocity methods. The dynamic phasor approach had been tested on the IEEE first benchmark SSR model, showing outstanding agreement with more computationally demanding alternative methods for eigenvalue analysis

2.2 Conclusions

In the present chapter comprehensive review of the development in the area of FACTS device like static synchronous series compensator and TCSC has been presented. It is observed that TCSC and IMDU are finding increasing application in the modern power system. A FLEXIBLE AC transmission is emerging as an advanced technology for the efficient utilization of existing power systems.

In the early stage of power system development, both steady state and transient stability problems challenged system planners. The development of fast acting static exciters and electronic voltage regulators overcame to large extend the transient stability and steady state problems (caused by slow shift in the generator rotor motion as the loading was increased).

Over the last few years, the problem of slow frequency oscillations has assumed importance. The frequency of oscillation in the range of 0.2 to 2.0 Hz. The lower the frequency, the more widespread are the oscillation (also called inter area oscillation). Another problem faced by modern power system is the problem of voltage collapse or voltage instability which is a manifestation of steady state instability. Historically steady

state instability has been associated with angle instability and slow loss of synchronism among generators .the slow collapse of voltage at load buses under high loading conditions and reactive power limitation is a recent phenomenon.

Power system bottlenecks are faced in countries with large generation reserves. The economic and environmental factors necessitate generation sites at remote location and wheeling of power through existing networks. The operational problem faced in such cases require detailed analysis of dynamic behavior of power system and development of suitable controllers to overcome the problem. For damping subsynchronous resonance phenomenon various FACT devices are available such as SVC, STATCOM, SSSC, TCSC, UPSC .

In my project I m using IMDU and TCSC device to damp SSR and finally to compare their relative merits and de-merits.

Chapter 3
SMALL-SIGNAL ANALYSIS OF SUBSYNCHRONOUS RESONANCE PHENOMENON

3.1 Introduction

The differential and algebraic equations which describe the dynamic performance of the synchronous machine and the transmission network are, in general, nonlinear. For the purpose of stability analysis, these equations may be linearized by assuming that a disturbance is considered to be small. Small-signal analysis using linear techniques provides valuable information about the inherent dynamic characteristics of the power system and assists in its design.

This chapter presents an analytical method useful in the study of small-signal analysis of subsynchronous resonance (SSR), establishes a linearized model for the power system, and performs the analysis of the SSR using the eigenvalue technique. by studying the small-signal stability of the power system, the engineer will be able to find countermeasures to damp all subsynchronous torsional oscillations.

3.2 IEEE First Benchmark Model Small Signal Analysis

The IEEE First Benchmark Model (FBM) [16] is developed by IEEE Subsynchronous Resonance Task Force for testing the various kinds of subsynchronous resonance countermeasures.

This system, shown in Figure 3.1, consists of a single series-capacitor compensated transmission line connecting a large turbine-generator to a large system. The shaft system of the turbine-generator unit consists of a high-pressure turbine (HP), an intermediate-pressure turbine (IP), two low pressure turbines (LPA & LPB), the generator rotor (GEN), and its rotating exciter (EXC).

This model offers various kinds of SSR problems and is chosen as a test system for testing the proposed SSR mitigation methods in this research work.

The schematic diagram of the FBM system is shown in Figure 3.1. The system mechanical and electrical data are given in Appendix B.

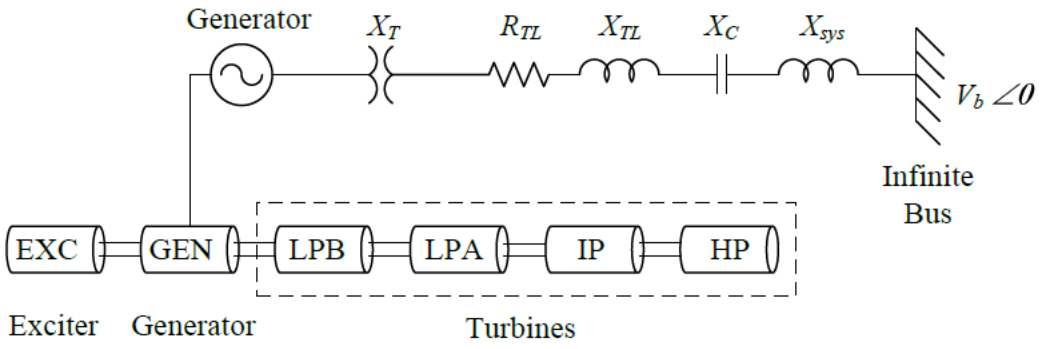

Figure 3.1 The IEEE First Benchmark Model schematic diagram.

3.3 Power System Modeling

The nonlinear differential equations of the system under study are derived by developing individually the mathematical models which represent the various components of the system.

The eigenvalue analysis gives information of both resonant frequency and damping at that frequency. So, to understand the effect of series compensation, a detailed mathematical model of the whole system is developed for eigenvalue analysis. First, individual mathematical models describing the synchronous generator, turbine-generator mechanical system, and electric network are presented. Then, all the equations are combined in a standard form for the computation of the eigenvalues.

3.3.1 Synchronous Machine Modeling

A conventional synchronous machine schematic diagram is shown in Figure 3.2 [21]. The model shows three-phase armature windings on the stator (*a, b,* and *c*). The rotor of the machine carries the field winding *fd* and damper windings. The damper windings are represented by equivalent damper circuits in the direct axis (*d*-axis) and quadrature axis (*q*-axis): *h* on *d*-axis, and *g* and *k* on *q*-axis.

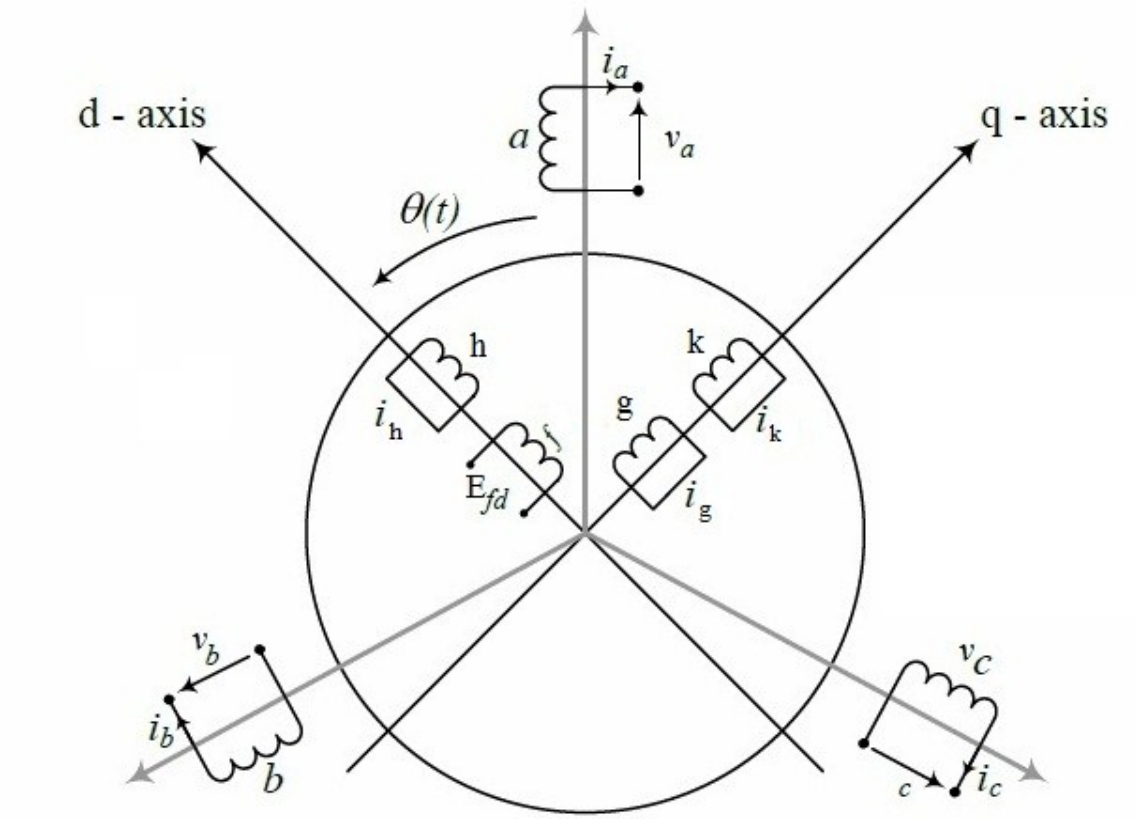

Figure 3.2 Schematic diagram of a conventional synchronous machine.

a,b,c	:	Stator windings
v_a,v_b,v_c	:	Stator three-phase winding voltages.
i_a,i_b,i_c	:	Stator three-phase winding currents.
f	:	Field winding.
E_{fd}	:	Field voltage.
h	:	d – axis damper winding.
g	:	First q – axis damper winding.
k	:	Second q – axis damper winding.
θ(t)	:	The electrical angle (in *rad*) by which *d* – axis leads magnetic axis of phase *a* winding.

Note: We will use Model 1.1[22] (Field circuit with one equivalent damper on q-axis) published by IEEE task force, of synchronous machine for modeling.

The electrical dynamic equations of the synchronous machine (model 1.1) are developed by writing equations of the coupled circuits and presented below [18-21]:

❖ ***Stator Equations:***

$$v_d = -\frac{1}{\omega_B}\frac{d\Psi_d}{dt} - (1+S_m)\Psi_q - R_a i_d \qquad \text{Eq. 3.1}$$

$$v_q = -\frac{1}{\omega_B}\frac{d\Psi_q}{dt} - (1+S_m)\Psi_d - R_a i_q \qquad \text{Eq. 3.2}$$

❖ ***Rotor Equations:***

$$\frac{dE_d'}{dt} = \frac{1}{T_{qo}'}\left[-E_d' - (x_q - x_q')i_q\right] \qquad \text{Eq. 3.3}$$

$$\frac{dE_q'}{dt} = \frac{1}{T_{do}'}\left[-E_q' + (x_d - x_d')i_d + E_{fd}\right] \qquad \text{Eq. 3.4}$$

Where

$$i_d = \frac{\Psi_d - E_q'}{x_d'} \quad \text{and} \quad i_q = \frac{\Psi_q + E_d'}{x_q'} \qquad \text{Eq. 3.5,3.6}$$

❖ ***Stator Flux Linkage Equations:***

$$\Psi_d = x_d i_d + x_{ad} i_f \qquad \text{Eq. 3.7}$$

$$\Psi_q = x_q i_q + x_{aq} i_g \qquad \text{Eq. 3.8}$$

❖ ***Rotor Flux linkage Equations:***

$$\Psi_f = x_{ad} i_d + x_f i_f \qquad \text{Eq. 3.9}$$

$$\Psi_g = x_{aq} i_q + x_g i_g \qquad \text{Eq. 3.10}$$

❖ ***Air-gap Torque Equation:***

$$T_e = \Psi_d i_q - \Psi_q i_d \qquad \text{Eq. 3.11}$$

Linearizing and rearranging Eq.3.1 to 3.6 and expressed as a set of first order differential equations as [18]:

$$\frac{d\Delta x_e}{dt} = [A_e]\Delta x_e + [B_{e1}]\Delta u_e + [B_{e2}]E_{fd} \qquad \text{Eq. 3.12}$$

And $$\Delta y_e = [C_e]\Delta x_e \qquad \text{Eq. 3.13}$$

Where

$$\left[\Delta \dot{x}_e\right]^t = \left[\Delta\dot{\Psi}_d \quad \Delta\dot{\Psi}_q \quad \Delta\dot{E}_d' \quad \Delta\dot{E}_q'\right]$$

$$\left[\Delta x_e\right]^t = \left[\Delta\Psi_d \quad \Delta\Psi_q \quad \Delta E_d' \quad \Delta E_q'\right]$$

$$\left[\Delta u_e\right]^t = \left[\Delta v_D \quad \Delta v_Q\right]$$

$$\left[\Delta y_e\right]^t = \left[\Delta i_D \quad \Delta i_Q\right]$$

$$[A_e] = \begin{bmatrix} -\frac{\omega_B R_a}{x_d'} & -\omega_B & 0 & \frac{\omega_B R_a}{x_d'} \\ \omega_B & -\frac{\omega_B R_a}{x_{q'}} & -\frac{\omega_B R_a}{x_q'} & 0 \\ 0 & -\frac{1}{T_{qo}'}\left(\frac{x_q}{x_q'} - 1\right) & -\frac{1}{T_{qo}'}\left(\frac{x_q}{x_q'}\right) & 0 \\ \frac{1}{T_{do}'}\left(\frac{x_d}{x_d'} - 1\right) & 0 & 0 & -\frac{1}{T_{do}'}\left(\frac{x_d}{x_d'}\right) \end{bmatrix}$$

$$[B_{e1}] = \begin{bmatrix} -\omega_B \cos\delta & \omega_B \sin\delta & 0 & 0 \\ -\omega_B \sin\delta & -\omega_B \cos\delta & 0 & 0 \\ 0 & 0 & 0 & 0 \\ 0 & 0 & 0 & 0 \end{bmatrix}$$

$$[B_{e2}]^t = \begin{bmatrix} 0 & 0 & 0 & \dfrac{1}{T_{do}'} \end{bmatrix}$$

$$[C_e] = \begin{bmatrix} \dfrac{\cos\delta}{x_d'} & \dfrac{\sin\delta}{x_q'} & \dfrac{\sin\delta}{x_q'} & -\dfrac{\cos\delta}{x_d'} \\ -\dfrac{\sin\delta}{x_d'} & \dfrac{\cos\delta}{x_q'} & \dfrac{\cos\delta}{x_q'} & \dfrac{\sin\delta}{x_d'} \end{bmatrix}$$

3.3.2 Modeling of Turbine Generator Mechanical System

The turbine-generator mechanical system consists of six masses; high-pressure turbine (HP), intermediate-pressure turbine (IP), low pressure turbine A (LPA) and low pressure turbine B (LPB), an exciter (EXC), and a generator (GEN) coupled to a common shaft as shown in Figure 3.3. The mechanical properties of the masses and shaft sections are given in Appendix B. The turbine masses, generator rotor and exciter are considered as lumped masses (rigid body) connected to each other via massless springs. The mathematical expressions describing the dynamics of the system are developed considering the lumped multi-mass model.

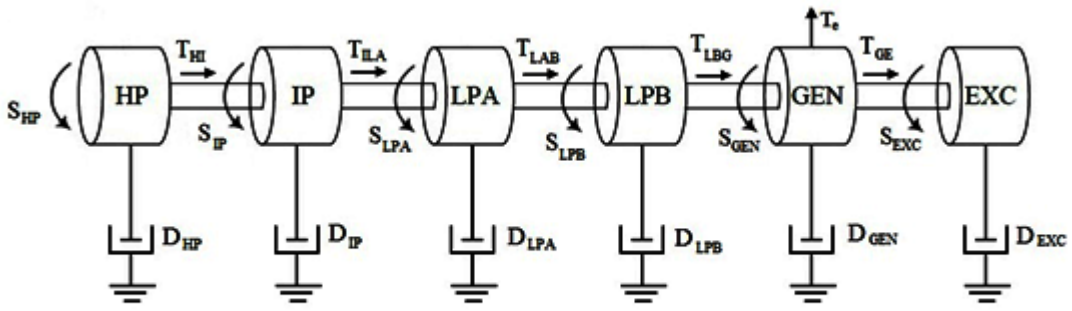

Figure 3.3 Mechanical structure of six mass FBM system.

Note: In the mechanical system we have considered *Slip* and *Torque* as state variables.

The mechanical system state space equations are[18]:

$$\dot{\delta}_{GEN} = S_{GEN}\omega_B \quad \text{Eq 3.14}$$

$$\dot{S}_{EXC} = -\frac{D_{EXC}}{2H_{EXC}} S_{EXC} + \frac{T_{GE}}{2H_{EXC}} \quad \text{Eq. 3.15}$$

$$\dot{T}_{GE} = K_{GE}\left(S_{GEN} - S_{EXC}\right) \quad \text{Eq.3.16}$$

$$\dot{S}_{GEN} = -\frac{D_{GEN}}{2H_{GEN}} S_{GEN} + \frac{1}{2H_{GEN}}\left(T_{LBG} - T_{GE}\right) - \frac{1}{2H_{GEN}} T_e \quad \text{Eq. 3.17}$$

$$\dot{T}_{LBG} = K_{LBG}\left(S_{LPB} - S_{GEN}\right) \quad \text{Eq. 3.18}$$

$$\dot{S}_{LPB} = -\frac{D_{LPB}}{2H_{LPB}} S_{LPB} + \frac{1}{2H_{LPB}}\left(T_{LAB} - T_{LBG}\right) \quad \text{Eq. 3.19}$$

$$\dot{T}_{LAB} = K_{LAB}\left(S_{LPA} - S_{LPB}\right) \quad \text{Eq. 3.20}$$

$$\dot{S}_{LPA} = -\frac{D_{LPA}}{2H_{LPA}} S_{LPA} + \frac{1}{2H_{LPA}}\left(T_{ILA} - T_{LAB}\right) \quad \text{Eq. 3.21}$$

$$\dot{T}_{ILA} = K_{ILA}\left(S_{IP} - S_{LPA}\right) \quad \text{Eq. 3.22}$$

$$\dot{S}_{IP} = -\frac{D_{IP}}{2H_{IP}} S_{IP} + \frac{1}{2H_{IP}}\left(T_{HI} - T_{ILA}\right) \quad \text{Eq. 3.23}$$

$$\dot{T}_{HI} = K_{HI}\left(S_{HP} - S_{IP}\right) \quad \text{Eq. 3.24}$$

$$\dot{S}_{HP} = -\frac{D_{HP}}{2H_{HP}} S_{HP} - \frac{T_{HI}}{2H_{HP}} \quad \text{Eq. 3.25}$$

Linearizing and rearranging Equation (3.14-3.25), the overall shaft equations can be given by the following matrix equation

$$\dot{\Delta x}_m = \left[A_m\right]\Delta x_m + \left[B_{m1}\right]\Delta T_e \quad \text{Eq. 3.26}$$

$$\Delta y_m = [C_m]\Delta x_m \qquad \text{Eq. 3.27}$$

Where:

$$\left[\dot{\Delta x}_m\right]^t = \left[\dot{\delta}_{GEN} \quad \dot{S}_{EXC} \quad \dot{T}_{GE} \quad \dot{S}_{GEN} \quad \dot{T}_{LBG} \quad \dot{S}_{LPB} \quad \dot{T}_{LAB} \quad \dot{S}_{LPA} \quad \dot{T}_{ILA} \quad \dot{S}_{IP} \quad \dot{T}_{HI} \quad \dot{S}_{HP}\right]$$

$$\left[\Delta x_m\right]^t = \left[\delta_{GEN} \quad S_{EXC} \quad T_{GE} \quad S_{GEN} \quad T_{LBG} \quad S_{LPB} \quad T_{LAB} \quad S_{LPA} \quad T_{ILA} \quad S_{IP} \quad T_{HI} \quad S_{HP}\right]$$

$$\left[\Delta y_m\right]^t = \left[\Delta\delta_{GEN} \quad \Delta S_{GEN}\right]$$

$$[B_{m1}] = \begin{bmatrix} 0 \\ 0 \\ 0 \\ -\dfrac{1}{2H_{GEN}} \\ 0 \\ 0 \\ 0 \\ 0 \\ 0 \\ 0 \\ 0 \\ 0 \end{bmatrix}$$

$$[C_m] = \begin{bmatrix} 1 & 0 & 0 & 0 & 0 & 0 & 0 & 0 & 0 & 0 & 0 & 0 \\ 0 & 0 & 0 & 1 & 0 & 0 & 0 & 0 & 0 & 0 & 0 & 0 \end{bmatrix}$$

$$[A_m] = \begin{bmatrix}
0 & 0 & 0 & \omega_B & 0 & 0 & 0 & 0 & 0 & 0 & 0 & 0 \\
0 & -\frac{D_{EXC}}{2H_{EXC}} & \frac{1}{2H_{EXC}} & 0 & 0 & 0 & 0 & 0 & 0 & 0 & 0 & 0 \\
0 & -K_{GE} & 0 & K_{GE} & 0 & 0 & 0 & 0 & 0 & 0 & 0 & 0 \\
0 & 0 & -\frac{1}{2H_{GEN}} & -\frac{D_{GEN}}{2H_{GEN}} & \frac{1}{2H_{GEN}} & 0 & 0 & 0 & 0 & 0 & 0 & 0 \\
0 & 0 & 0 & -K_{LBG} & 0 & K_{LBG} & 0 & 0 & 0 & 0 & 0 & 0 \\
0 & 0 & 0 & 0 & -\frac{1}{2H_{LPB}} & -\frac{D_{LPB}}{2H_{LPB}} & \frac{1}{2H_{LPB}} & 0 & 0 & 0 & 0 & 0 \\
0 & 0 & 0 & 0 & 0 & -K_{LAB} & 0 & K_{LAB} & 0 & 0 & 0 & 0 \\
0 & 0 & 0 & 0 & 0 & 0 & -\frac{1}{2H_{LPA}} & -\frac{D_{LPA}}{2H_{LPA}} & \frac{1}{2H_{LPA}} & 0 & 0 & 0 \\
0 & 0 & 0 & 0 & 0 & 0 & 0 & -K_{ILA} & 0 & K_{ILA} & 0 & 0 \\
0 & 0 & 0 & 0 & 0 & 0 & 0 & 0 & -\frac{1}{2H_{IP}} & -\frac{D_{IP}}{2H_{IP}} & \frac{1}{2H_{IP}} & 0 \\
0 & 0 & 0 & 0 & 0 & 0 & 0 & 0 & 0 & -K_{HI} & 0 & K_{HI} \\
0 & 0 & 0 & 0 & 0 & 0 & 0 & 0 & 0 & 0 & -\frac{1}{2H_{HP}} & -\frac{D_{HP}}{2H_{HP}}
\end{bmatrix}$$

Now in Eq. 3.11, putting values of ψ_d and ψ_q from 3.7,3.8 and on linearizing T_e we get:

$$[\Delta T_e] = [C_{me}]\Delta x_e \qquad \text{Eq. 3.28}$$

Where:

$$[C_{me}]^t = \begin{bmatrix} \dfrac{(x_d' - x_q')}{x_d' x_q'}\Psi_{qo} + \dfrac{E_{do}'}{x_q'} \\ \dfrac{(x_d' - x_q')}{x_d' x_q'}\Psi_{do} + \dfrac{E_{qo}'}{x_d'} \\ \dfrac{\Psi_{do}}{x_q'} \\ \dfrac{\Psi_{qo}}{x_d'} \end{bmatrix}$$

From Eq. 3.28 and 3.26

$$\dot{\Delta x}_m = [B_{m1}C_{me}]\Delta x_e + [A_m]\Delta x_m \qquad \text{Eq. 3.29}$$

3.3.3 Synchronous M/C Mechanical and Electrical System Combined Equation

Modified electrical system equations are

$$\dot{\Delta x}_e = [A_e]\Delta x_e + [B_{e1}]\Delta u_e + [B_{e2}]E_{fd} + [B_{e3}]\Delta y_m \qquad \text{Eq. 3.30}$$

From Eq. 3.27

$$\dot{\Delta x}_e = [A_e]\Delta x_e + [B_{e3}C_m]\Delta x_m + [B_{e1}]\Delta u_e + [B_{e2}]E_{fd} \qquad \text{Eq. 3.31}$$

Combining Eq. 3.31 and 3.29

$$\dot{\Delta x}_G = [A_G]\Delta x_G + [B_{G1}]\Delta u_g + [B_{G2}]E_{fd} \qquad \text{Eq. 3.32}$$

Where;

$$\left[\dot{\Delta x}_G\right]^t = \left[\dot{\Delta x}_e \quad \dot{\Delta x}_m\right]$$

$$\left[\Delta x_G\right]^t = \left[\Delta x_e \quad \Delta x_m\right]$$

$$[B_{e3}] = \begin{bmatrix} \omega_B v_{qo} & -\omega_B \Psi_{qo} \\ -\omega_B v_{do} & \omega_B \Psi_{do} \\ 0 & 0 \\ 0 & 0 \end{bmatrix}$$

$$[A_G] = \begin{bmatrix} [A_e] & [B_{e3}C_m] \\ [B_{m1}C_{me}] & [A_m] \end{bmatrix}$$

$$[B_{G1}] = \begin{bmatrix} B_{e1} \\ 0 \end{bmatrix}$$

$$[B_{G2}] = \begin{bmatrix} B_{e2} \\ 0 \end{bmatrix}$$

And also modified output equation:

$$\Delta y_G = [C_e]\Delta x_e + [C_{em}]\Delta y_m \qquad \text{Eq. 3.33}$$

From Eq. 3.27

$$\Delta y_G = [C_e]\Delta x_e + [C_{em}C_m]\Delta x_m \qquad \text{Eq. 3.34}$$

$$\Delta y_G = [C_G]\Delta x_G \qquad \text{Eq. 3.35}$$

Where:

$$[\Delta y_G] = \begin{bmatrix} \Delta i_D \\ \Delta i_Q \end{bmatrix}$$

$$[C_G] = [[C_E] \quad [C_{em}C_m]]$$

$$[C_{em}] = [P_{em}]\begin{bmatrix} x_{eo} & \underline{0} \end{bmatrix}$$

$$[P_{em}] = \left[\frac{\Delta C_e}{\Delta \delta}\right] = \begin{bmatrix} -\frac{\sin\delta}{x_d'} & \frac{\cos\delta}{x_q'} & \frac{\cos\delta}{x_q'} & \frac{\sin\delta}{x_d'} \\ -\frac{\cos\delta}{x_d'} & -\frac{\sin\delta}{x_q'} & -\frac{\sin\delta}{x_q'} & \frac{\cos\delta}{x_d'} \end{bmatrix}$$

$$\left[x_{eo}\right]^t = \begin{bmatrix} \Psi_{do} & \Psi_{qo} & E_{do}' & E_{qo}' \end{bmatrix}$$

So final combined electrical and mechanical equations are

$$\dot{\Delta x}_G = [A_G]\Delta x_G + [B_{G1}]\Delta u_g + [B_{G2}]E_{fd} \qquad \text{Eq. 3.36}$$

$$\Delta y_G = [C_G]\Delta x_G \qquad \text{Eq. 3.37}$$

3.3.4 Modeling of the Transmission Line

A series capacitor-compensated transmission line may be represented by the *RLC* circuit [18] shown in Figure 3.4.

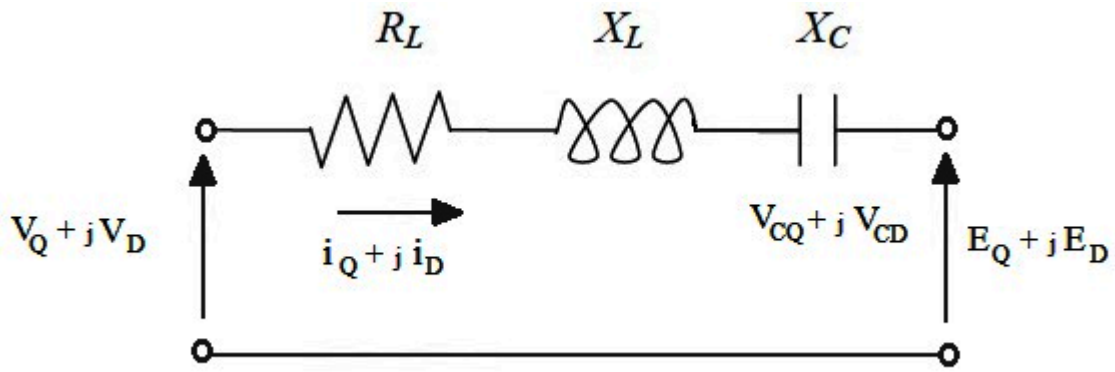

Figure 3.4 A series capacitor-compensated transmission line.

Note: We will take voltage across capacitor as state variable.

The differential equations for the circuit elements, after applying Park's transformation, can be expressed in the d-q reference frame as following

The voltage across the capacitor [18]:

$$\begin{bmatrix} \Delta\dot{V}_{CD} \\ \Delta\dot{V}_{CQ} \end{bmatrix} = \begin{bmatrix} 0 & -\omega_B \\ \omega_B & 0 \end{bmatrix} \begin{bmatrix} \Delta Vc_D \\ \Delta Vc_Q \end{bmatrix} + \begin{bmatrix} \omega_B X_C & 0 \\ 0 & \omega_B X_C \end{bmatrix} \begin{bmatrix} \Delta i_D \\ \Delta i_Q \end{bmatrix}$$

The above equations can be represented in state space model as:

$$\Delta\dot{x}_N = [A_N]\Delta x_N + [B_{N1}]\Delta u_{N1} + [B_{N2}]\Delta u_{N2} \qquad \text{Eq. 3.38}$$

Where:

$$[\Delta\dot{x}_N]^t = \begin{bmatrix} \Delta\dot{V}_{CD} & \Delta\dot{V}_{CQ} \end{bmatrix}$$

$$[U_{N1}] = \begin{bmatrix} i_D \\ i_Q \end{bmatrix}$$

$$[U_{N2}] = \begin{bmatrix} E_D \\ E_Q \end{bmatrix}$$

$$[A_N] = \begin{bmatrix} 0 & -\omega_B \\ \omega_B & 0 \end{bmatrix}$$

$$[B_{N1}] = \begin{bmatrix} \omega_B X_C & 0 \\ 0 & \omega_B X_C \end{bmatrix}$$

$$[B_{N2}] = [0]$$

3.3.5 Combined Generator and Transmission Line Modeling

The combined system equations can be obtain after eliminating the variables u_e and u_{N1}.

Since $$u_{N1} = y_G = [C_G] x_G$$ Eq. 3.39

And the expression for u_e depends upon the network.

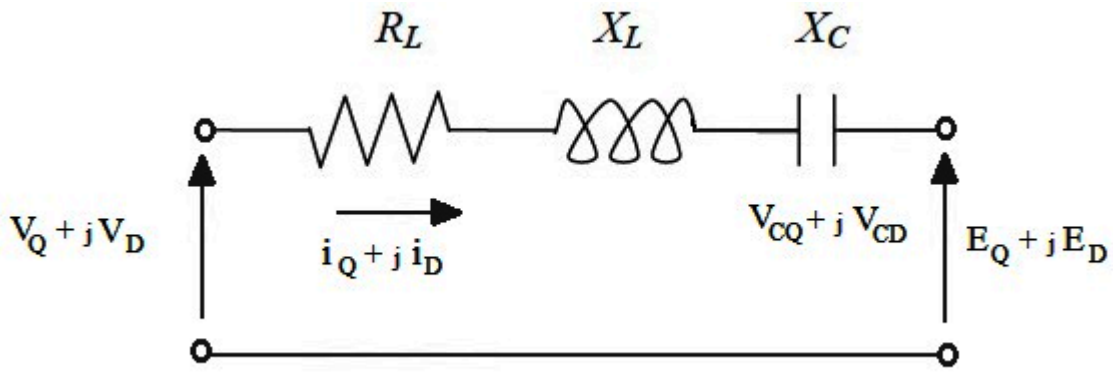

Figure 3.5 Network Diagram

For the network as shown in figure 3.5, we have

$$V_D = E_D + V_{CD} + Ri_D + \frac{X_L}{\omega_B}\dot{i}_D + X_L i_Q$$ Eq. 3.40

$$V_Q = E_Q + V_{CQ} + Ri_Q + \frac{X_L}{\omega_B}\dot{i}_Q + X_L i_D$$ Eq. 3.41

From equation 3.40, 3.41, 3.32 and 3.35 and on linearzing we have

$$\Delta u_e = [H]\left[\Delta x_N + [F_1]\Delta x_G + \frac{X_L}{\omega_B}[C_G B_{G2}]\Delta E_{fd} + \Delta u_{N2}\right] \qquad \text{Eq. 3.42}$$

Where:

$$[H] = \left\{I - \frac{X_L}{\omega_B}[C_G B_{G1}]\right\}^{-1}$$

I *is a unit matrix.*

$$[F_1] = [FC_G] + \frac{X_L}{\omega_B}[C_G A_G]$$

$$[F] = \begin{bmatrix} R & X_L \\ -X_L & R \end{bmatrix}$$

From Equation 3.36 and 3.42, the final System equations are:

$$\dot{\Delta x}_T = [A_T]\Delta x_T + [B_{T1}]\Delta E_{fd} + [B_{T2}]\Delta u_{N2} \qquad \text{Eq. 3.43}$$

Where:

$$\left[\dot{\Delta x}_T\right]^t = \begin{bmatrix} \dot{\Delta x}_G & \dot{\Delta x}_N \end{bmatrix}$$

$$\left[\Delta x_T\right]^t = \begin{bmatrix} \Delta x_G & \Delta x_N \end{bmatrix}$$

$$[A_T] = \begin{bmatrix} [A_G] + [B_{G1}HF_1] & [B_{G1}H] \\ [B_{N1}C_G] & [A_N] \end{bmatrix}$$

$$[B_{T1}] = \begin{bmatrix} [B_{G2}] + \frac{X_L}{\omega_B}[B_{G1}HC_G B_{G2}] \\ 0 \end{bmatrix}$$

$$[B_{T2}] = \begin{bmatrix} [B_{G1}H] \\ [B_{N2}] \end{bmatrix}$$

3.3.6 Simulation of IEEE First Benchmark Model

The above system is simulated with the help of MATLAB. The Nework parameter are based on generator base of 892.4 MVA are given in Appendix B .The Synchronous M/C data are given in Appendix B.The shaft inertia and spring constant are given in Appendix B. There are six inertia corresponding to six rotors in which there are four turbines, one generator and one rotating exciter.

The generator is assumed to be operated at 0.7 pu load(P_G=0.7). The infinite bus voltage is assumed to be 1.0 pu. The AVR is neglected in the study. The nominal value of series compensation is assumed to be 70% (X_C=0.35 pu). Damping is assumed to zero

Table 3.1 Eigenvalues of the combined system

S.No.	Machine Model(1.1) P=0.7, P.F.=0.9	Comments
1	-0.46505 + j10.128 -0.46505 – j10.128	Torsional Mode #0
2	0.043375 + j99.574 0.043375 – j99.574	Torsional Mode #1
3	0.028616 + j127.13 0.028616 – j127.13	Torsional Mode #2
4	0.03606 + j160.34 0.03606 – j160.34	Torsional Mode #3
5	0.001427 + j202.85 0.001427 – j202.85	Torsional Mode #4
6	-2.879e-07 + j298.18 -2.879e-07 - j298.18	Torsional Mode #5
7	-3.3979 + j141.26 -3.3979 – j141.26	Network Mode #1
8	-4.4197 + j612.42 -4.4197 – j612.42	Network Mode #2
9	-0.083245	
10	-4.0937	

It is obvious from the Table 3.1 that when the electrical network subsynchronous resonance frequency is near to one of the torsional modes , the corresponding torsional mode is destabilized.

3.4 Time Domain Analysis

The above IEEE FBM was studied for small signal stability in time domain with the help of SIMULINK available in the MATLAB.

SIMULINK model was made and it was given step input as:

$\mathbf{E_{fd} = 1}$

$\mathbf{V_{cd} = 1}$

$\mathbf{V_{cq} = 1}$

And following observations were obtained (till 10 seconds) :

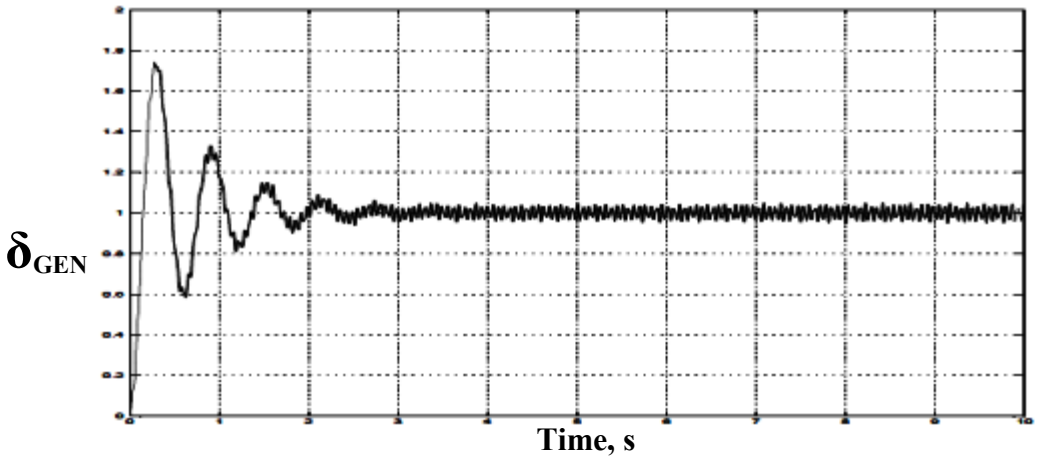

Figure 3.6 Variation of torque angle with time (X_C=0.35)

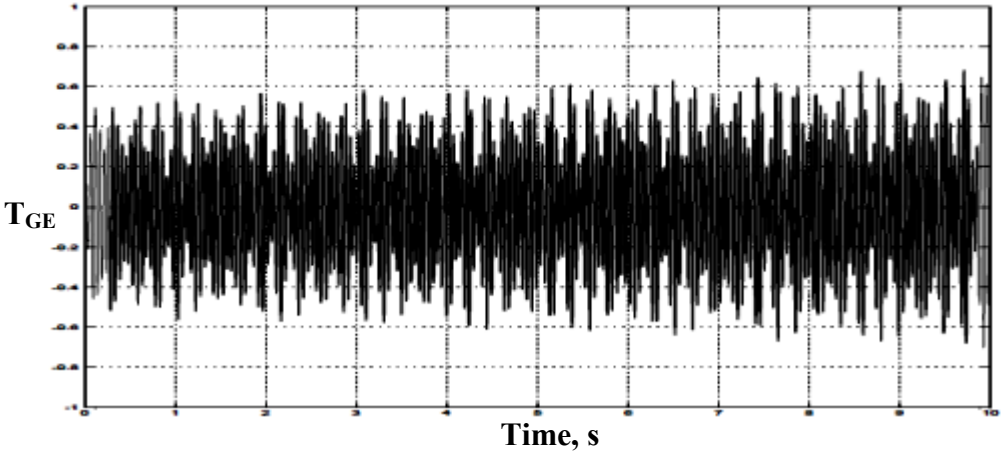

Figure 3.7 Variation of torque at GE shaft with time (X_C=0.35)

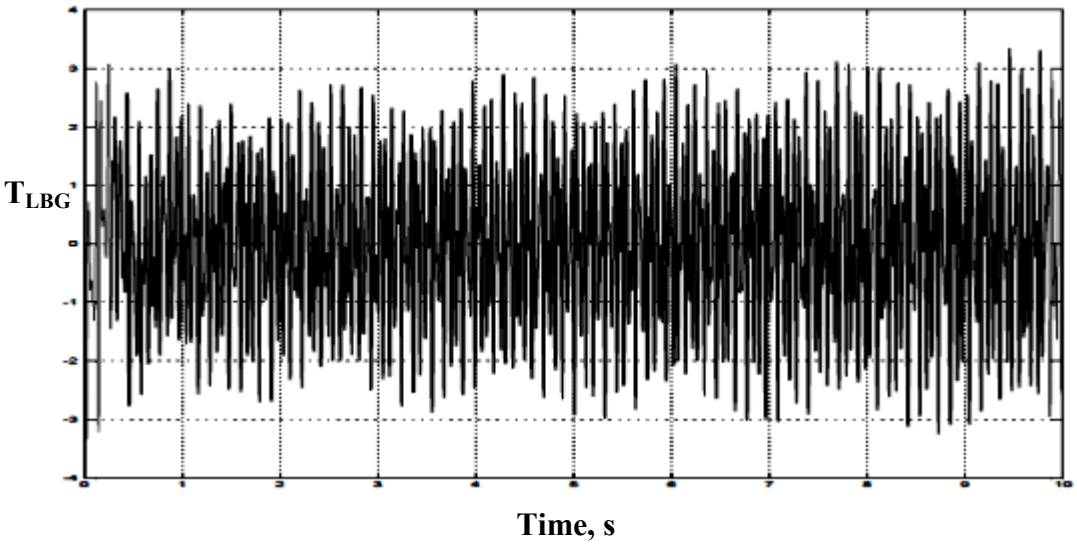

Figure 3.8 Variation of torque at LBG shaft with time (X_C=0.35)

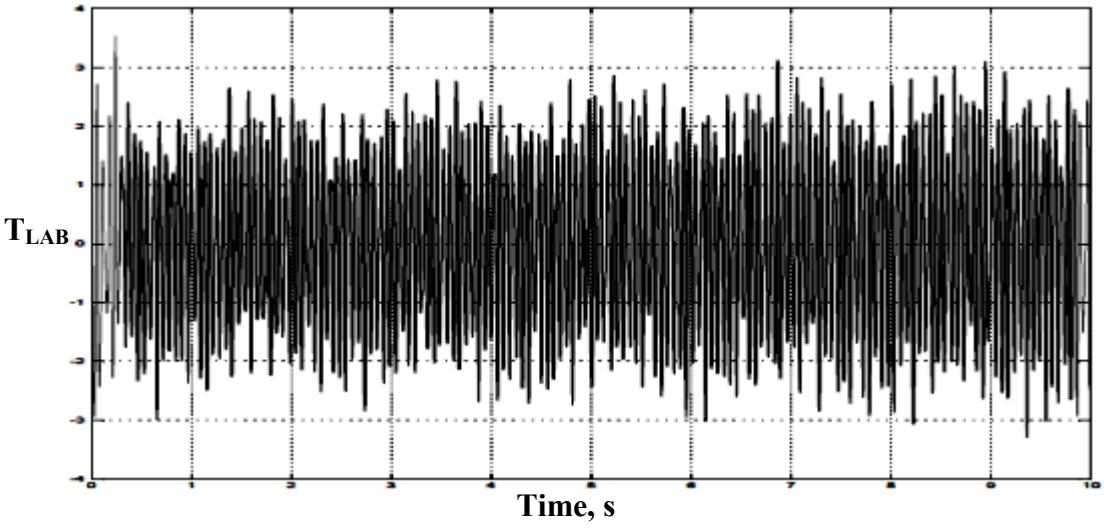

Figure 3.9 Variation of torque at LAB shaft with time (X_C=0.35)

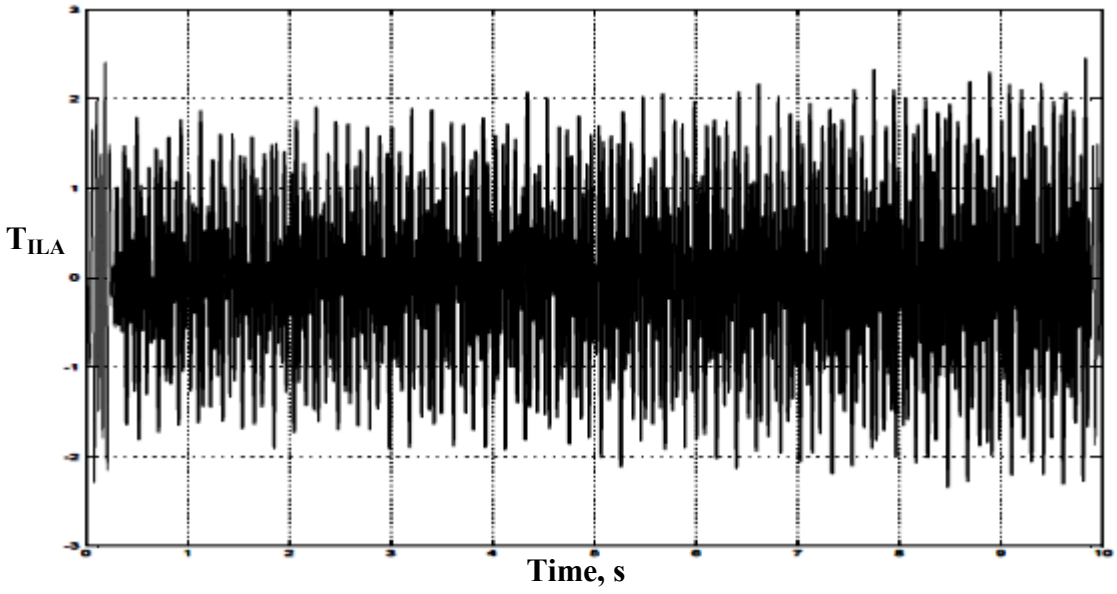

Figure 3.10 Variation of torque at ILA shaft with time (X_C=0.35)

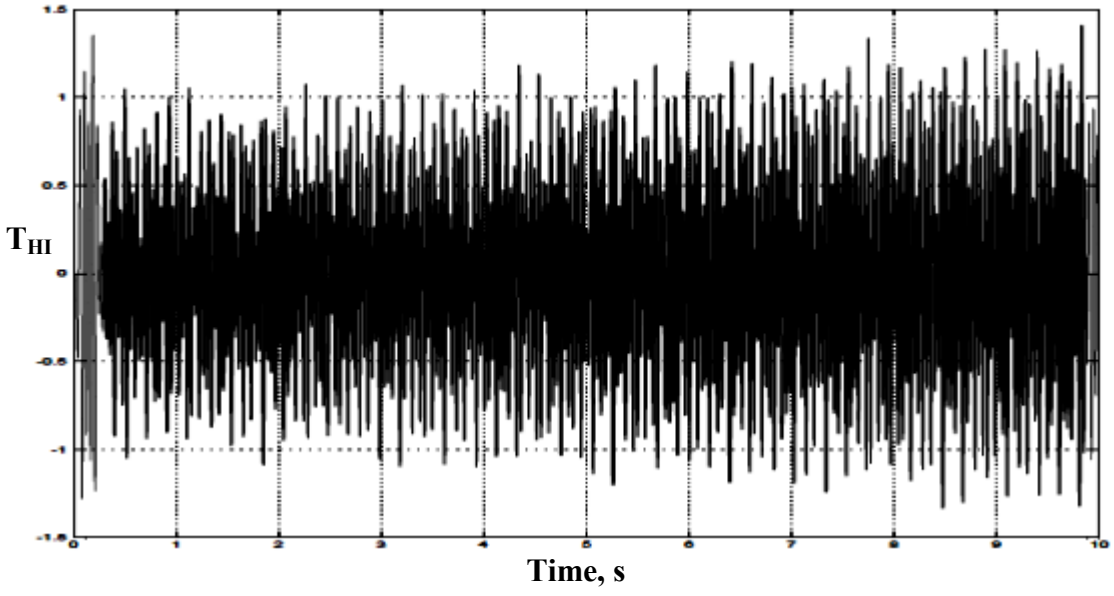

Figure 3.11 Variation of torque at HI shaft with time (X_C=0.35)

3.5 Summary

This chapter presented the investigations of the subsynchronous resonance phenomenon under small disturbances. These investigations are conducted on the IEEE first benchmark model which consists of a large turbine-generator connecting to an infinite bus system through a series capacitor compensated transmission line.

The analysis was performed by modeling the individual systems (synchronous generator, electric network, and turbine-generator mechanical system) separately. The dynamic equations are linearized and combined in a single expression. These set of linearized equations were grouped and mathematically manipulated in order to obtain the overall system model in a state-space form.

It is observed that the mechanical system exhibits five modes of torsional oscillations. In many cases, reducing the compensation level can solve the torsional interaction problem, but is not an economic solution.

The analysis shows that the FBM system is suitable for testing the robustness of the proposed technique.

Chapter 4

DAMPING SUBSYNCHRONOUS RESONANCE USING INDUCTION MACHINE DAMPING UNIT

4.1 Introduction:

The problem of torsional oscillations occurs because of active power imbalance (a difference between turbine input and generator output) during rotor swing, but only little work has been reported for handling this problem through active power control.

The damping unit is an induction machine running at synchronous speed during steady state, consequently consuming or generating no power. In fact, it can even be electrically disconnected, drawing no magnetizing current.

The property of an induction machine to act either as a generator or motor is utilized to absorb mechanical power if there is excess and to release it when there is a deficiency.

High pressure (HP) and other turbines produce torque in the direction of rotation (forward direction) and the generator produces the electromagnetic torque in the opposite direction.

The T-G set has a long shaft and consequently the turbine and generator torques produce an angular twist in the shaft. The twist angle is dependent on load, and during steady-state operation it is constant. However, during the torsional oscillating state the angle varies periodically. If the system has negative damping, the amplitude of the torsional oscillations will grow exponentially which may damage the shaft.

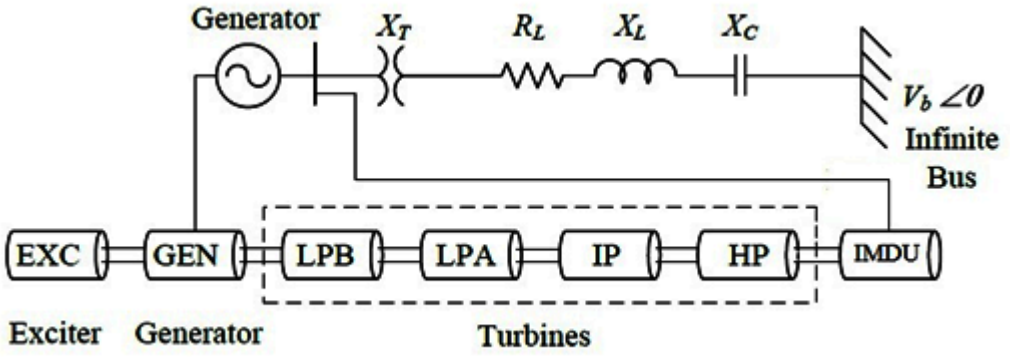

Figure 4.1 IMDU Connected to the System

If an induction machine is connected to the HP turbine on its right side as shown in Fig. 4.1 and if the speed of the machine exceeds the synchronous speed (mechanical input is greater than electrical output of generator) the machine acts as an induction generator. Torque produced by it is in the reverse direction. It can be visualized that this torque will tend to reduce the twist angle (δ), hence it reduces the amplitude of torsional oscillation. Alternatively, it can be said that it increases the damping of the system.

If the speed of the shaft is less than the synchronous speed, the induction machine will act as a motor and it produces a torque in the forward direction. In this operation, it supports the turbine torque and helps to restore the speed.

So in any case it tries to oppose the change in the synchronous speed of the shaft. It can be said that it reduces the oscillations in the rotating mass around the nominal speed, or that the damping of the system is increased.

Since this machine comes into operation during transients only, it is designed for very high short-term rating and very small continuous rating; consequently the machine has low inertia, low power, small size and low cost.

Because of its small mass and tight coupling with the high pressure turbine it has been considered a single mass unit with the HP turbine. Electrically it is connected to the generator bus.

4.2 Modeling the Induction Machine Damping Unit

For the eigenvalue analysis, the torque-speed characteristics of an induction machine, with small rotor resistance, to be used as IMDU can be considered linear between synchronous speed and the critical slip (maximum torque) when operated at constant terminal voltage and frequency. Therefore, the torque of the damping unit can be modeled as being proportional to speed deviation, (deviation from synchronous speed). The slope of the torque-speed characteristic found as [15]:

$$k = \left| \frac{\Delta T_{IM}}{\Delta \omega_{IM}} \right|$$

The IMDU interaction with the generator mechanical system is illustrated in Fig. 4.2. The field exciter dynamics is not modeled and the excitation is held constant at 1 pu. The time constant of the mechanical system is very large when compared to the electrical system, and hence, the speed governor dynamics are not included, keeping the

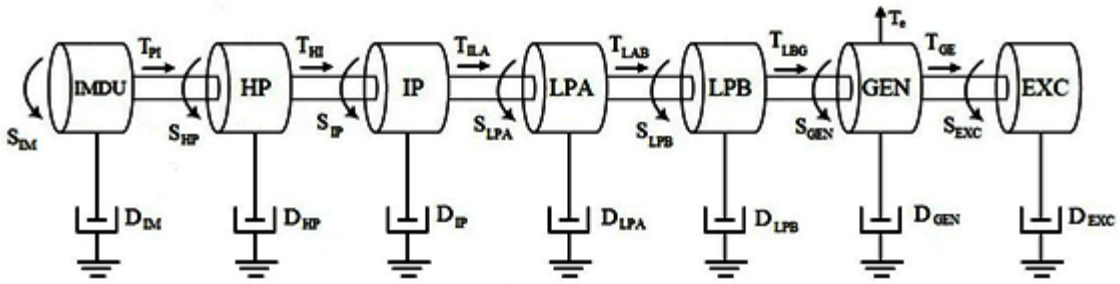

Figure 4.2 IMDU under Speed Operation

input power to the turbines constant. Variables torque produced in the different shaft section, which are functions of the difference of the slip at the ends of the shaft.

The differential equations governing the IMDU model of Fig. 4.2 are as follows [15]:

$$\dot{T}_{PI} = K_{PI}\left(S_{IM} - S_{HP}\right) \qquad \text{Eq. 4.1}$$

$$\dot{S}_{IM} = -\frac{D_{IM} - k}{2H_{IM}} S_{IM} - \frac{T_{PI}}{2H_{IM}} \qquad \text{Eq. 4.2}$$

Also Eq. 3.25 is modified to

$$\dot{S}_{HP} = -\frac{D_{HP}}{2H_{HP}} S_{HP} + \frac{1}{2H_{HP}}\left(T_{PI} - T_{HI}\right) \qquad \text{Eq. 4.3}$$

The network consider is same as before

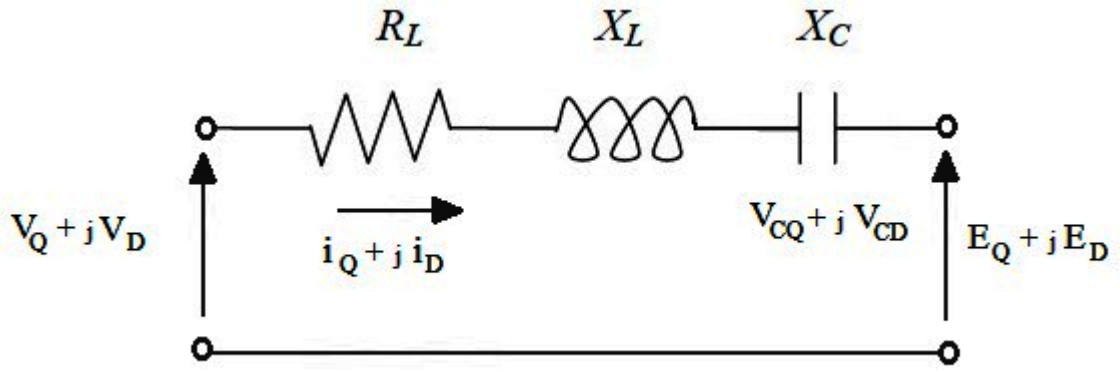

Figure 4.3 A series capacitor-compensated transmission line.

So modified mechanical system can be described as

$$\Delta \dot{x}_{mI} = [A_{mI}]\Delta x_{mI} + [B_{m1}]\Delta T_e \qquad \text{Eq. 4.4}$$

$$\Delta y_m = [C_{mI}]\Delta x_{mI} \qquad \text{Eq. 4.5}$$

Where

$$\left[\Delta \dot{x}_{mI}\right]^t = \left[\dot{\delta}_{GEN} \quad \dot{S}_{EXC} \quad \dot{T}_{GE} \quad \dot{S}_{GEN} \quad \dot{T}_{LBG} \quad \dot{S}_{LPB} \quad \dot{T}_{LAB} \quad \dot{S}_{LPA} \quad \dot{T}_{ILA} \quad \dot{S}_{IP} \quad \dot{T}_{HI} \quad \dot{S}_{HP}\dot{T}_{PI} \quad \dot{S}_{IM}\right]$$

$$\left[\Delta x_{mI}\right]^t = \left[\delta_{GEN} \quad S_{EXC} \quad T_{GE} \quad S_{GEN} \quad T_{LBG} \quad S_{LPB} \quad T_{LAB} \quad S_{LPA} \quad T_{ILA} \quad S_{IP} \quad T_{HI} \quad S_{HP}T_{PI} \quad S_{IM}\right]$$

$$[B_{m1}] = \begin{bmatrix} 0 \\ 0 \\ 0 \\ -\frac{1}{2H_{GEN}} \\ 0 \\ 0 \\ 0 \\ 0 \\ 0 \\ 0 \\ 0 \\ 0 \\ 0 \\ 0 \end{bmatrix}$$

$$[C_m] = \begin{bmatrix} 1 & 0 & 0 & 0 & 0 & 0 & 0 & 0 & 0 & 0 & 0 & 0 & 0 & 0 \\ 0 & 0 & 0 & 1 & 0 & 0 & 0 & 0 & 0 & 0 & 0 & 0 & 0 & 0 \end{bmatrix}$$

$$
[A_m] = \begin{bmatrix}
0 & 0 & 0 & \omega_B & 0 & 0 & 0 & 0 & 0 & 0 & 0 & 0 & 0 & 0 \\
0 & -\frac{D_{EXC}}{2H_{EXC}} & \frac{1}{2H_{EXC}} & 0 & 0 & 0 & 0 & 0 & 0 & 0 & 0 & 0 & 0 & 0 \\
0 & -K_{GE} & 0 & K_{GE} & 0 & 0 & 0 & 0 & 0 & 0 & 0 & 0 & 0 & 0 \\
0 & 0 & -\frac{1}{2H_{GEN}} & -\frac{D_{GEN}}{2H_{GEN}} & \frac{1}{2H_{GEN}} & 0 & 0 & 0 & 0 & 0 & 0 & 0 & 0 & 0 \\
0 & 0 & 0 & -K_{LBG} & 0 & K_{LBG} & 0 & 0 & 0 & 0 & 0 & 0 & 0 & 0 \\
0 & 0 & 0 & 0 & -\frac{1}{2H_{LPB}} & -\frac{D_{LPB}}{2H_{LPB}} & \frac{1}{2H_{LPB}} & 0 & 0 & 0 & 0 & 0 & 0 & 0 \\
0 & 0 & 0 & 0 & 0 & -K_{LAB} & 0 & K_{LAB} & 0 & 0 & 0 & 0 & 0 & 0 \\
0 & 0 & 0 & 0 & 0 & 0 & -\frac{1}{2H_{LPA}} & -\frac{D_{LPA}}{2H_{LPA}} & \frac{1}{2H_{LPA}} & 0 & 0 & 0 & 0 & 0 \\
0 & 0 & 0 & 0 & 0 & 0 & 0 & -K_{ILA} & 0 & K_{ILA} & 0 & 0 & 0 & 0 \\
0 & 0 & 0 & 0 & 0 & 0 & 0 & 0 & -\frac{1}{2H_{IP}} & -\frac{D_{IP}}{2H_{IP}} & \frac{1}{2H_{IP}} & 0 & 0 & 0 \\
0 & 0 & 0 & 0 & 0 & 0 & 0 & 0 & 0 & -K_{HI} & 0 & K_{HI} & 0 & 0 \\
0 & 0 & 0 & 0 & 0 & 0 & 0 & 0 & 0 & 0 & -\frac{1}{2H_{HP}} & -\frac{D_{HP}}{2H_{HP}} & \frac{1}{2H_{HP}} & 0 \\
0 & 0 & 0 & 0 & 0 & 0 & 0 & 0 & 0 & 0 & 0 & -K_{PI} & 0 & K_{PI} \\
0 & 0 & 0 & 0 & 0 & 0 & 0 & 0 & 0 & 0 & 0 & 0 & -\frac{1}{2H_{IM}} & -\frac{D_{IM}-k}{2H_{IM}}
\end{bmatrix}
$$

Now new A_G

$$[A_{GI}] = \begin{bmatrix} [A_e] & [B_{e3}C_m] \\ [B_{m1}C_{me}] & [A_{mI}] \end{bmatrix}$$

And the final system equations are

$$\dot{\Delta x}_{TI} = [A_{TI}]\Delta x_{TI} + [B_{T1}]\Delta E_{fd} + [B_{T2}]\Delta u_{N2} \qquad \text{Eq. 4.6}$$

Where:

$$\left[\dot{\Delta x}_{TI}\right]^t = \left[\dot{\Delta x}_{GI} \quad \dot{\Delta x}_N\right]$$

$$\left[\Delta x_{TI}\right]^t = \left[\Delta x_{GI} \quad \Delta x_N\right]$$

$$[A_{TI}] = \begin{bmatrix} [A_{GI}] + [B_{G1}HF_1] & [B_{G1}H] \\ [B_{N1}C_G] & [A_N] \end{bmatrix}$$

4.3 Simulation of IEEE First Benchmark with IMDU

The FBS system is simulated with the help of MATLAB. The Network parameter are based on generator base of 892.4 MVA are given in Appendix B .The Synchronous M/C data are given in Appendix B.The shaft inertia and spring constant are given in Appendix B. There are six inertia corresponding to six rotors in which there are four turbines, one generator and one rotating exciter. Table 4.1 shows eigenvalues obtained.

The generator is assumed to be operated at 0.7 pu load (P_G=0.7). The infinite bus voltage is assumed to be 1.0 pu. The AVR is neglected in the study. The nominal value of series compensation is assumed to be 70% (X_C=0.35 pu). Damping is assumed to zero. The IMDU is coupled to HP and electrical connected to System. The IMDU data is provided in Appendix B.

Table 4.1 Eigenvalues of the combined system with IMDU

S.No.	Machine Model(1.1) P=0.7 ,P.F.=0.9	Comments
1	-0.88054 + j10.081 -0.88054 – j10.081	Torsional Mode #0
2	-2.33 + j96.698 -2.33 - j96.698	Torsional Mode #1
3	-0.59096 + j126.27 -0.59096 – j126.27	Torsional Mode #2
4	-5.0673 + j147.1 -5.0673 – j147.1	Torsional Mode #3
5	-0.27956 + j201.61 -0.27956 – j201.61	Torsional Mode #4
6	-2.1094 + j286.73 -2.1094 – j286.73	Torsional Mode #5
7	-2.7704 + j142.04 -2.7704 - j142.04	Network Mode #1
8	-4.4197 + j612.42 -4.4197 - j612.42	Network Mode #2
9	-0.082673	
10	-4.0916	
11	-23.67 + j737.19 -23.67 – j737.19	IMDU

4.4 Location of IMDU

IMDU is used for damping SSR, and it is mechanically connected to turbine system. IMDU can be connected to either HP end of T-G shaft or between any of the shaft segment i.e. HP-IP, IP-LPA, LPA-LPB. We conduct eigenvalue analysis with IMDU located at different positions along the T-G shaft and perform a comparative study in which coupling coefficient between IMDU and various shaft segments were kept at the same values and also the slope K (ratio of torque to speed) was also fixed.

Table 4.2 shows the different eigenvalues for different IMDU locations. From the eigenvalue analysis we see that the eigenvalues for the IMDU connected at the HP shaft end has highest real negative part. So IMDU connected at the HP end of T-G shaft damp SSR most effectively. For the connection of IMDU between HP and IP, all eigenvalues has real negative part but they have less real negative part as compared to IMDU connected to HP end, and for the rest of the cases one of the eigenvalues has real positive part, so the system becomes unstable.

So the best location for IMDU connection is to the HP end of the turbine-Generator shaft.

Table 4.2 Eigenvalues of the combined system with different IMDU locations

S. No	IMDU at HP end	IMDU between HP and IP end	IMDU between IP an LPA	IMDU between LPA an LPB	Comments
1	-0.88 + j10.1 -0.88 – j10.1	-0.88 + j10.1 -0.88 - j10.1	-0.87 + j10.1 -0.87 - j10.1	-0.87 + j10.1 -0.87 - j10.1	Torsional Mode #0
2	-2.33 + j96.7 -2.33 - j96.7	-1.28 + j98.5 -1.28 - j 98.5	-0.61 + j98.7 -0.61 - j98.7	-0.01 + j88.1 -0.01 - j88.1	Torsional Mode #1
3	-0.59 + j126.27 -0.59 – j126.27	-0.17 + j127.1 -0.17 - j127.1	-0.02 + j127.1 -0.02 - j127.1	0.001 + j126.1 0.001 - j126.1	Torsional Mode #2
4	-5.06 + j147.1 -5.06 – j147.1	-3.31 + j141.2 -3.31 - j141.2	-3.38 + j141.3 -3.38 - j141.3	-3.35 + j141.4 -3.35 - j141.4	Torsional Mode #3
5	-0.28 + j201.6 -0.28 – j201.6	-0.23 + j204.6 -0.23 - j 204.6	-0.06 + j202.7 -0.06 - j202.7	-0.07 + j191.8 -0.07 - j191.8	Torsional Mode #4
6	-2.11 + j286.7 -2.11 – j286.7	-0.01 + j368.7 -0.01 - j368.7	-1.14 + j294.3 -1.14 - j294.3	-0.01 + j297.7 -0.01 - j297.7	Torsional Mode #5
7	-2.77 + j142.1 -2.77 - j142.1	-2.42 + j165.1 -2.42 - j165.1	0.02 + j160.7 0.02 - j160.7	-0.12 + j158.9 -0.12 - j158.9	Network Mode #1
8	-4.42 + j612.4 -4.42 - j612.4	-4.42 + j612.4 -4.42 - j612.4	-4.42 + j612.4 -4.42 - j612.4	-4.42 + j612.4 -4.42 - j612.4	Network Mode #2
9	-0.082	-0.082	-0.082	-0.082	
10	-4.09	-4.09	-4.09	-4.09	
11	-23.67 + j737.2 -23.67 – j737.2	-29.38 + j946.4 -29.38 - j946.4	-31.62 + j912.1 -31.62 - j912.1	-33.27 + j890.9 -33.27 - j890.9	IMDU

4.5 Time Domain Analysis

The above Model was studied for small signal stability in time domain with the help of SIMULINK available in the MATLAB.

SIMULINK model was made and it was given step input as(for 10 sec):

$\mathbf{E_{fd} = 1}$

$\mathbf{V_{cd} = 1}$

$\mathbf{V_{cq} = 1}$

And following observations were obtained:

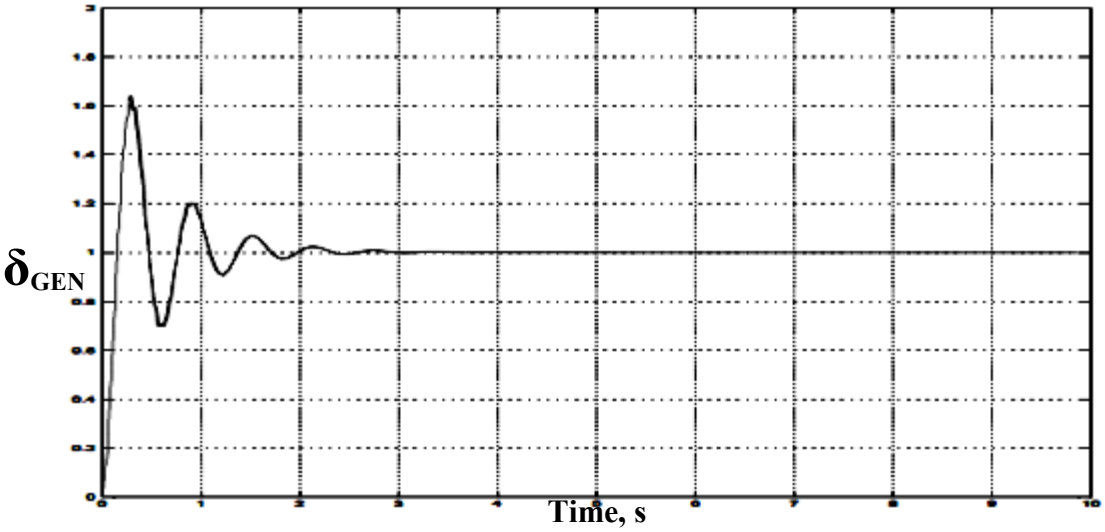

Figure 4.4 Variation of torque angle with time (with IMDU)

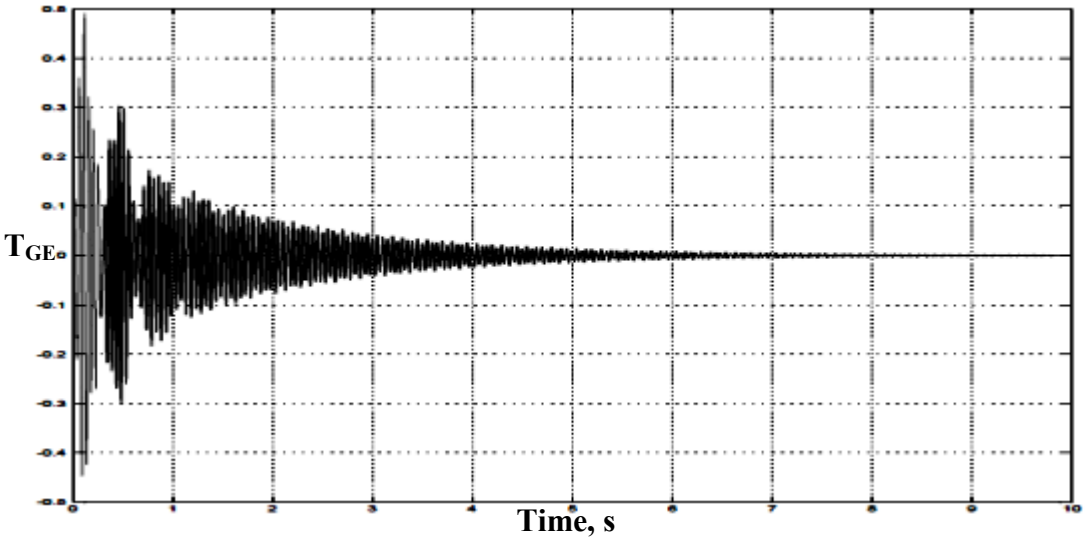

Figure 4.5 Variation of torque at GE shaft with time (with IMDU)

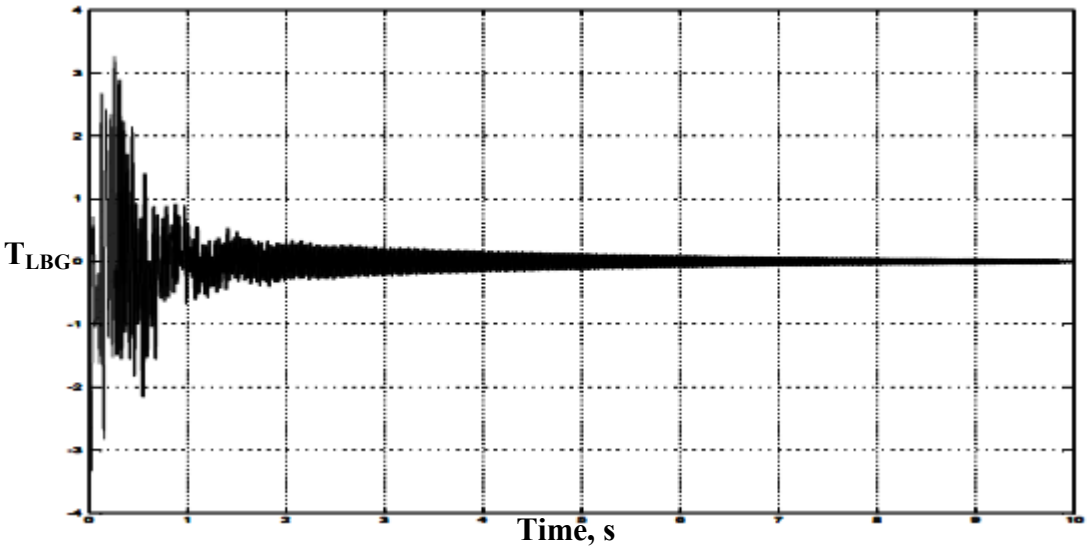

Figure 4.6 Variation of torque at LBG shaft with time (with IMDU)

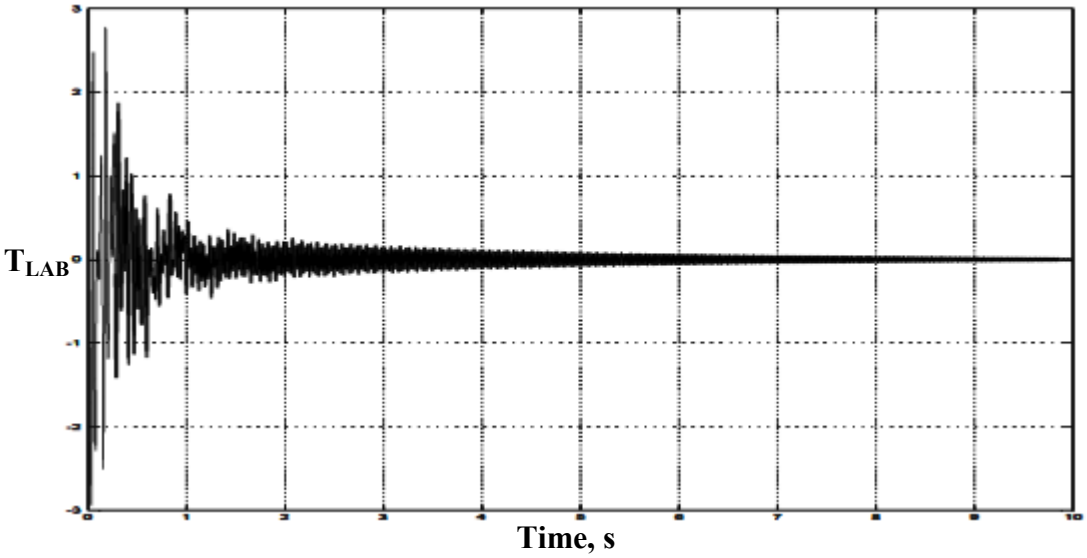

Figure 4.7 Variation of torque at LAB shaft with time (with IMDU)

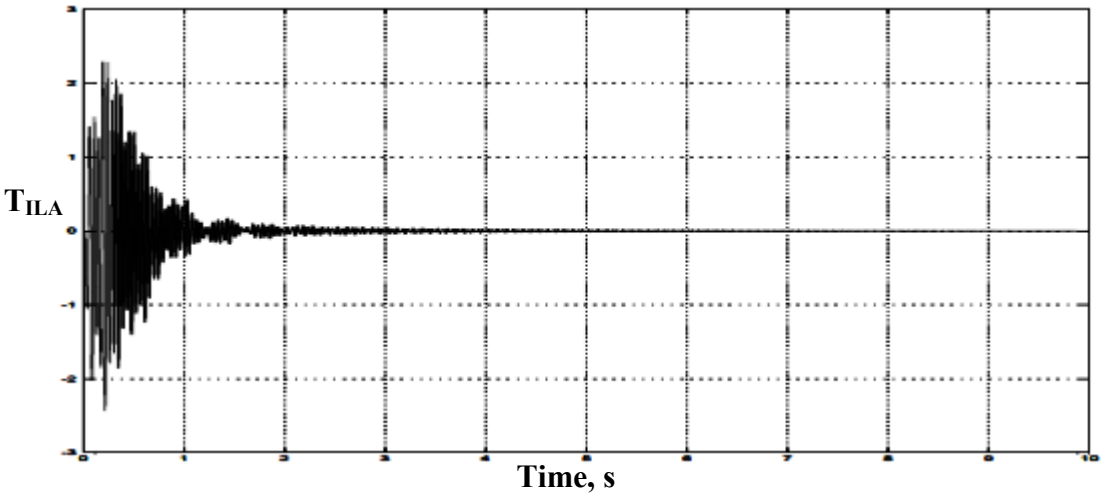

Figure 4.8 Variation of torque at ILA shaft with time (with IMDU)

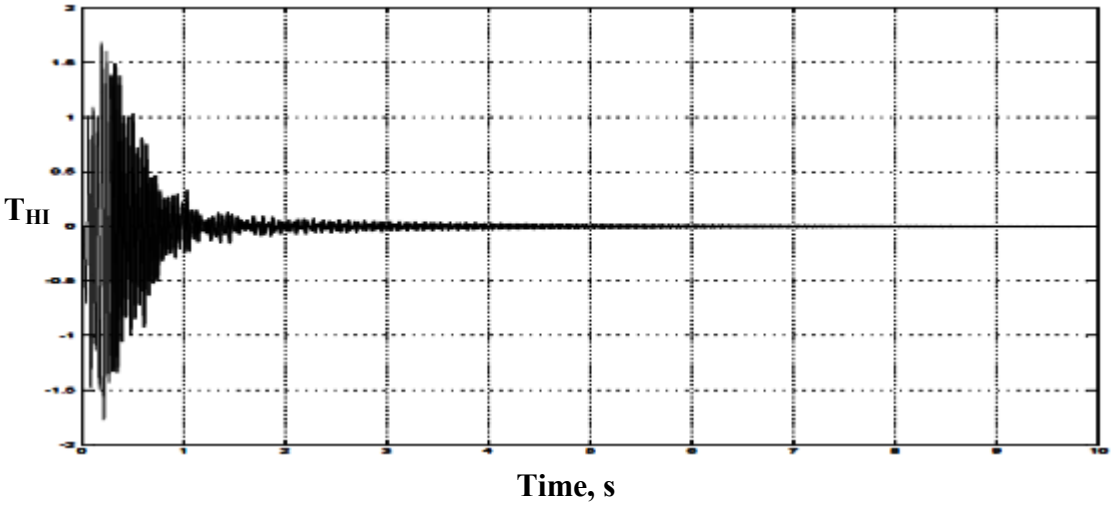

Figure 4.9 Variation of torque at HI shaft with time (with IMDU)

4.6 Summary

This chapter presented the investigations of the subsynchronous resonance damping using IMDU under small disturbances. These investigations are conducted on the IEEE first benchmark model which consists of a large turbine-generator connecting to an infinite bus system through a series capacitor compensated transmission line.

The analysis was performed by modeling the individual systems (synchronous generator, electric network, and turbine-generator mechanical system) separately. The dynamic equations are linearized and combined in a single expression. These set of linearized equations were grouped and mathematically manipulated in order to obtain the overall system model in a state-space form.

It is observed that the IMDU provides sufficient damping torque to the system to mitigate sub-synchronous phenomenon.

Chapter 5

DAMPING SUBSYNCHRONOUS RESONANCE USING THYRISTOR CONTROLLED SERIES CAPACITOR

5.1 Introduction

Series compensation of long lines using fixed capacitors is an economic solution to the problem of enhancing power transfer and improving system stability. However series compensated transmission lines connected to turbo generators can result in SSR due to negative damping introduced by the electrical network. This can cause self excitation due to torsional interaction (TI) and induction generator effect (IGE). The reduction of damping at torsional frequencies can also result in magnification of shaft torque oscillations caused by transient disturbances.

The hybrid series compensation consisting of suitable combination of passive elements and FACTS controllers such as TCSC or SSSC can be used to mitigate SSR.

TCSC is presented with the analysis of a system based on IEEE FBM. The linear analysis (based on the D-Q model) considers only the dynamic phasors representing fundamental frequency components in the network, ignoring harmonics introduced by the switching action.

Thyristor-controlled series capacitor (TCSC) consists of a series capacitor shunted by a thyristor-controlled reactor. A schematic diagram of the TCSC is shown in Figure 5.1. In practical implementations, several such compensators are connected in series to obtain the desired voltage rating and operating characteristics.

The basic purpose of the TCSC scheme is to provide continuously variable capacitor compensation by means of partially canceling the effective compensating capacitance by the TCR.

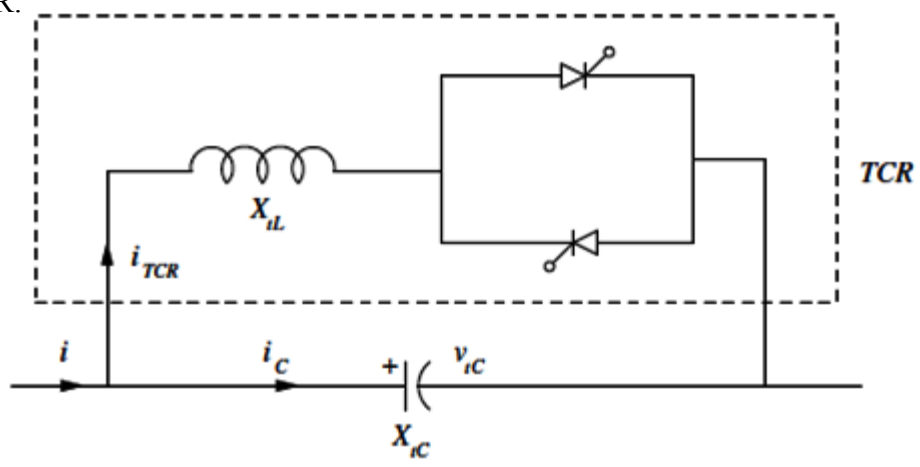

Figure 5.1 Schematic Diagram of TCSC

5.2 Modeling the TCSC

The schematic of TCSC attached to system is shown in Fig. 5.2. The TCSC is modelled in detail taking into consideration of the switching action of thyristors for transient simulation.

The eigenvalue analysis is based on the dynamic phasor model of TCSC given in reference [24], where the TCSC is modelled as a variable capacitor.

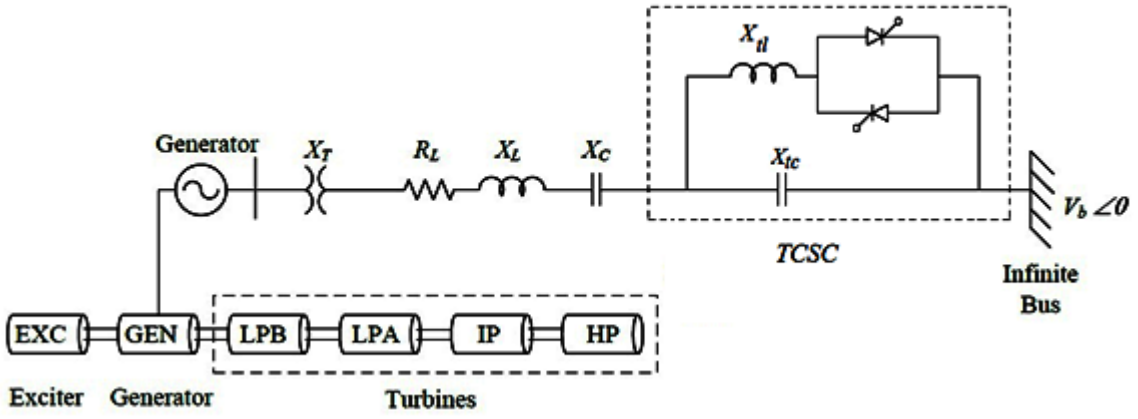

Figure 5.2 IEEE First Benchmark Model with TCSC compensation

The equations of TCSC in D-Q frame of reference can be given as [24]

$$\frac{dV_{tCD}}{dt} = (I_D - b_{Ceff} V_{tCQ}) \frac{\omega_B}{b_{ctc}} \qquad \text{Eq. 5.1}$$

$$\frac{dV_{tCQ}}{dt} = (I_Q + b_{Ceff} V_{tCD}) \frac{\omega_B}{b_{ctc}} \qquad \text{Eq. 5.2}$$

Where

$$b_{ctc}(p.u.) = C_{tc}(p.u.) = \frac{1}{X_{tc}}(p.u.)$$

$$b_{Ceff}(p.u.) = C_{eff}(p.u.)$$

$$L_{tl}(p.u.) = X_{tl}(p.u.)$$

$$C_{eff}(\sigma) = \left[\frac{1}{C_{tC}} - \frac{4}{\pi} \left\{ \frac{1}{2C_{tC}} \frac{1}{1-k_t^{-2}} \left(\frac{\sigma}{2} + \frac{\sin(\sigma)}{2} \right) + \frac{\omega_r L_{tL} S k_t}{k_t^2 - 1} \cos^2\left(\frac{\sigma}{2}\right) \left(\tan\left(\frac{\sigma}{2}\right) - k_t \tan\left(\frac{k_t \sigma}{2}\right) \right) \right\} \right]^{-1} \qquad \text{Eq. 5.3}$$

Where

$$\omega_r = \sqrt{\frac{1}{C_{tC} L_{tL}}}$$

$$S = \frac{1}{1 - k_t^{-2}}$$

$$k_t = \sqrt{\frac{X_{tC}}{X_{tL}}}$$

The prevailing conduction angle σ can be approximated as

$$\begin{aligned} \sigma &= \sigma^* + 2\phi \\ &\approx \sigma^* + 2\arg[-jI\overline{V_{tC}}] \\ &= \sigma^* + 2\arg[(I_D V_{tCQ} - I_Q V_{tCD}) - j(I_Q V_{tCQ} - I_D V_{tCD})] \end{aligned} \qquad \text{Eq. 5.4}$$

Where $\sigma^* = \pi - 2\alpha^*$ is the conduction angle reference .

From equations 3.31, 3.38, 3.35, 3.42, 5.1, 5.2

$$\dot{\Delta x}_T = [A_T]\Delta x_T + [B_{T1}]\Delta E_{fd} + [B_{T2}]\Delta u_{N2} \qquad \text{Eq. 5.5}$$

Where

$$\left[\dot{\Delta x}_T\right]^t = \begin{bmatrix} \dot{\Delta x}_G & \dot{\Delta x}_N & \dot{\Delta x}_{TCSC} \end{bmatrix}$$

$$\left[\Delta x_T\right]^t = \begin{bmatrix} \Delta x_G & \Delta x_N & \Delta x_{TCSC} \end{bmatrix}$$

$$[A_T]=\begin{bmatrix} [A_G]+[B_{G1}HF_1] & [B_{G1}H] & [B_{G1}H] \\ [B_{N1}C_G] & A_N & B_{N2} \\ F_1 * C_G & 0 & F_2 \end{bmatrix}$$

$$[B_{T2}]=\begin{bmatrix} [B_{G1}H] \\ [B_{N2}] \end{bmatrix}$$

$$[B_{T1}]=\begin{bmatrix} [B_{G2}]+\frac{X_L}{\omega_B}[B_{G1}HC_GB_{G2}] \\ 0 \end{bmatrix}$$

Where

$$F_1=\begin{bmatrix} \frac{\omega_B}{b_{ctc}} & 0 \\ 0 & \frac{\omega_B}{b_{ctc}} \end{bmatrix}$$

$$F_2=\begin{bmatrix} 0 & -\frac{b_{Ceff}}{b_{ctc}}\omega_B \\ \frac{b_{Ceff}}{b_{ctc}}\omega_B & 0 \end{bmatrix}$$

5.3 Simulation of IEEE First Benchmark with TCSC

The FBS system is simulated with the help of MATLAB. The Network parameter are based on generator base of 892.4 MVA are given in Appendix B.

The generator is assumed to be operated at 0.7 pu load (P_G=0.7) and at 0.9 lagging P.F. The infinite bus voltage is assumed to be 1.0 pu. The AVR is neglected in the study. The nominal value of series compensation is assumed to be (X_C=0.5 pu).

Table 5.1 Eigenvalues of the combined system with TCSC

S.No.	Machine Model(1.1) P=0.7, P.F.=0.9, X_{TCSC}=0.20	Comments
1	-1.0409 + j14.162 -1.0409 - j14.162	Torsional Mode #0
2	-0.25793 + j98.237 -0.25793 – j98.237	Torsional Mode #1
3	-1.316 + j126.98 -1.316 – j126.98	Torsional Mode #2
4	-0.33452 + j160.54 -0.33452 – j160.54	Torsional Mode #3
5	-0.085585 + j202.9 -0.085585 – j202.9	Torsional Mode #4
6	-0.36358 + j298.18 -0.36358 – j298.18	Torsional Mode #5
7	-1.8704 + j67.84 -1.8704 – j67.84	Network Mode #1
8	-0.48833 + j497.65 -0.48833 – j497.65	Network Mode #2
9	-6.1563	
10	-0.1718	
11	-3.8336+ j733.5 -3.8336 - j733.5	TCSC

5.4 Time Domain Analysis

The above Model was studied for small signal stability in time domain with the help of SIMULINK available in the MATLAB.

SIMULINK model was made and it was given step input as (for 10 sec):

$\mathbf{E_{fd} = 1}$

$\mathbf{V_{cd} = 1}$

$\mathbf{V_{cq} = 1}$

And following observations were obtained:

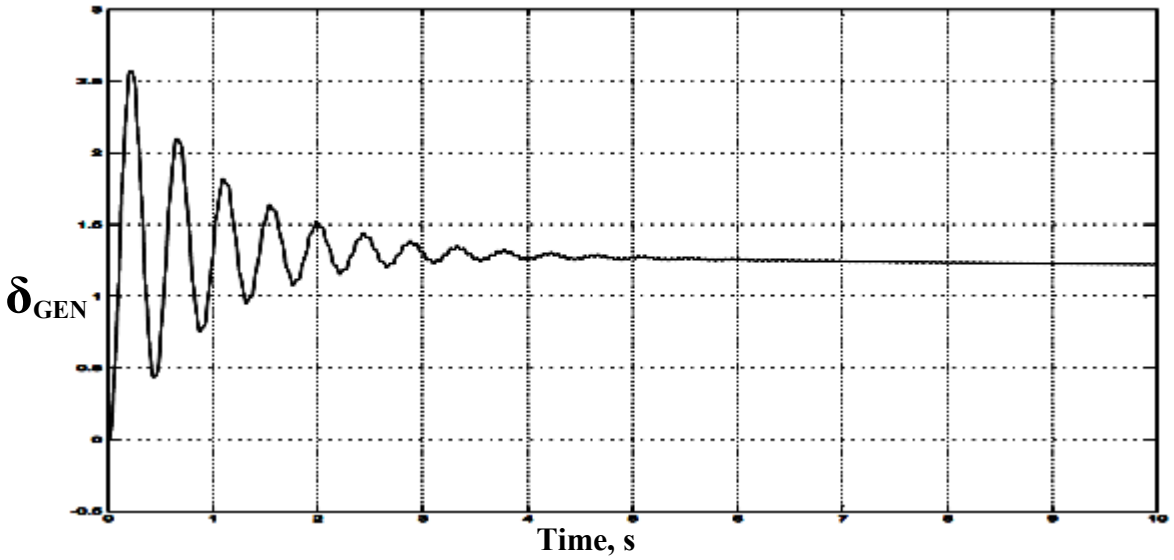

Figure 5.3 Variation of torque angle with time (with TCSC)

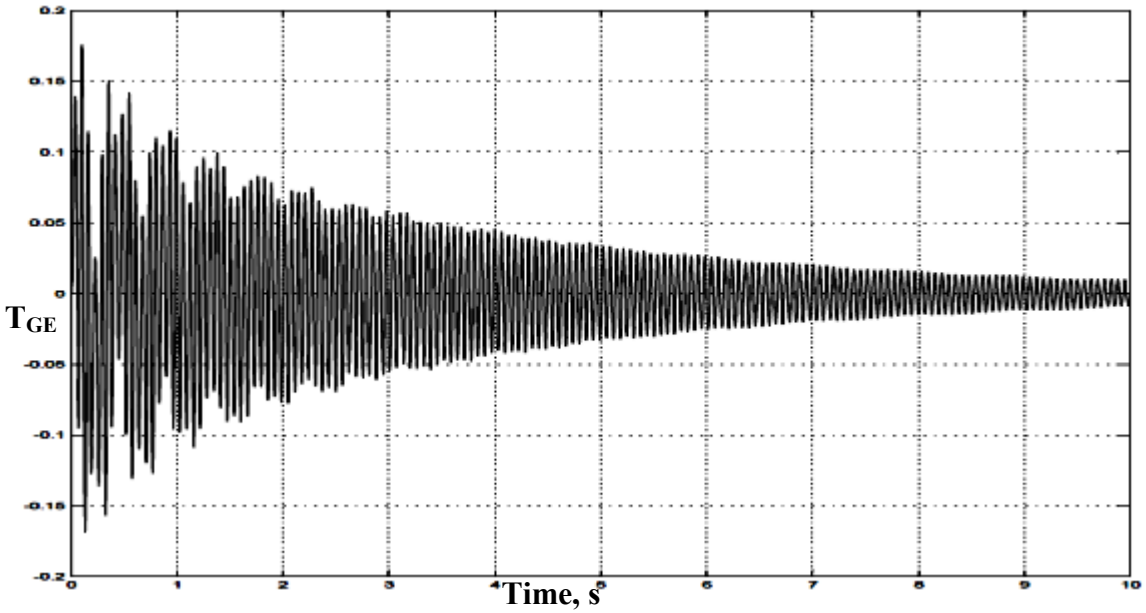

Figure 5.4 Variation of torque at GE shaft with time (with TCSC)

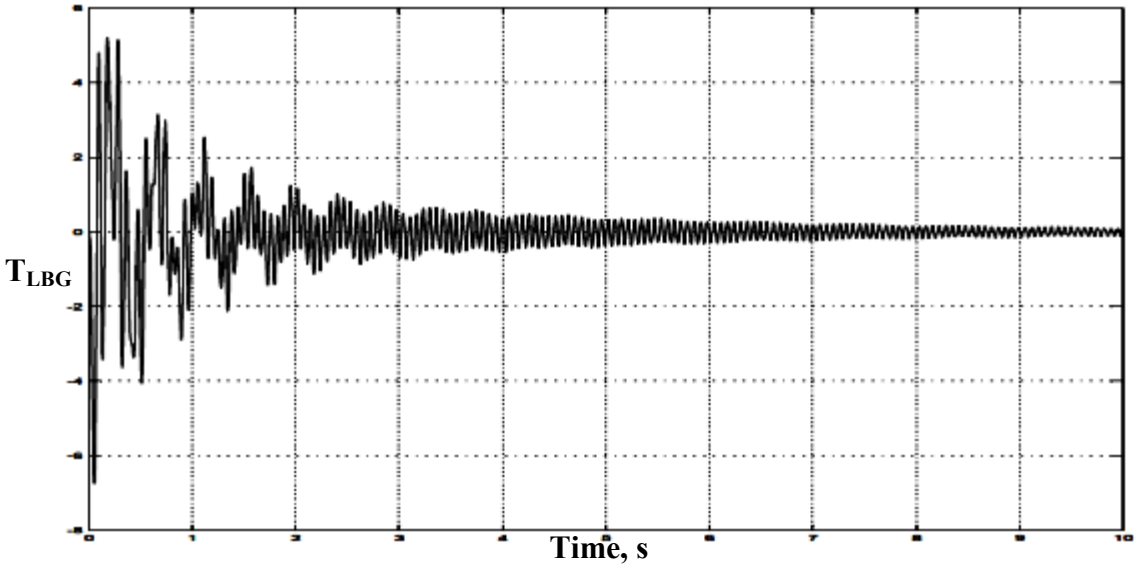

Figure 5.5 Variation of torque at LBG shaft with time (with TCSC)

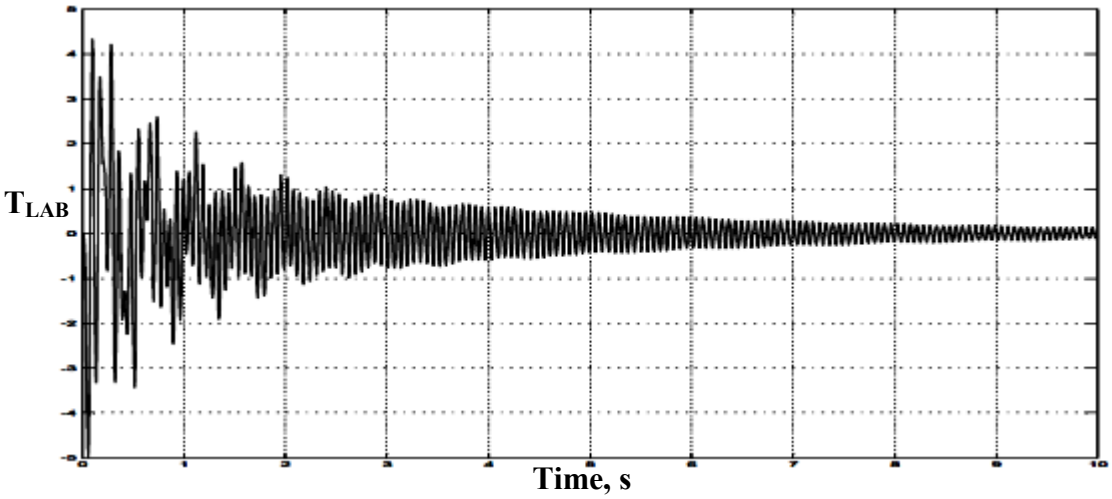

Figure 5.6 Variation of torque at LAB shaft with time (with TCSC)

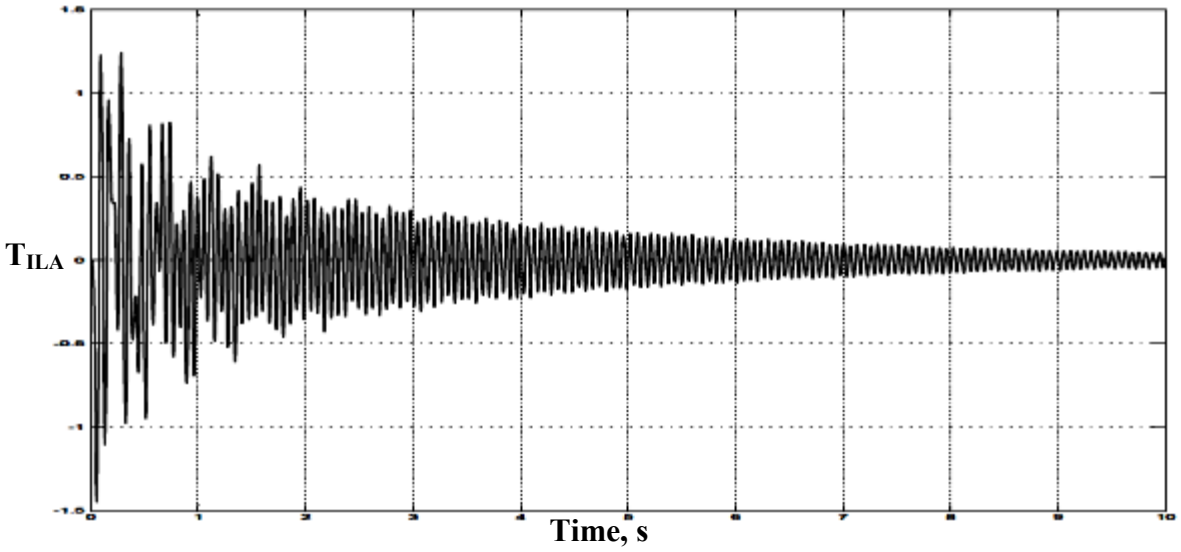

Figure 5.7 Variation of torque at ILA shaft with time (with TCSC)

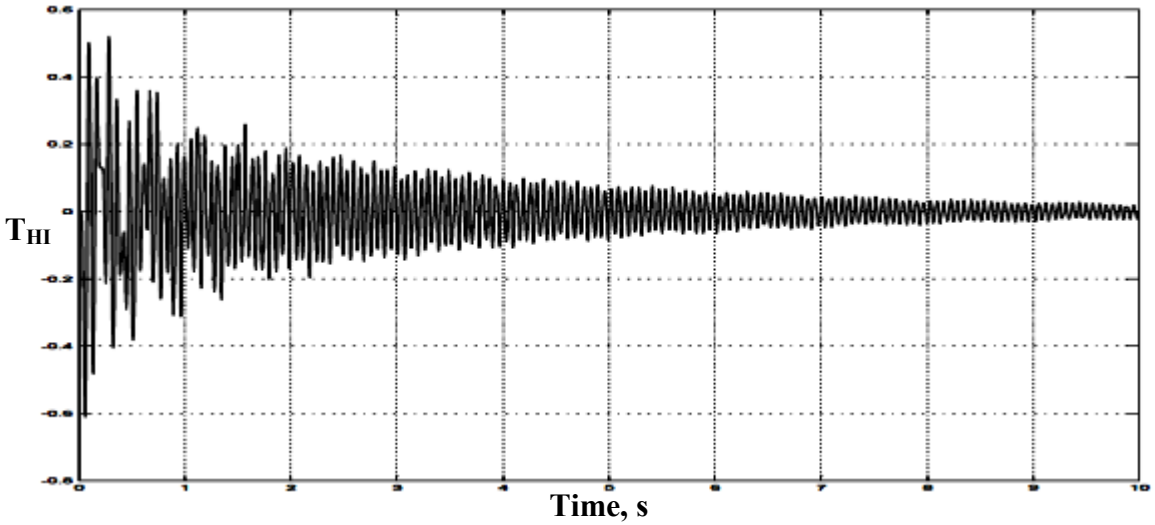

Figure 5.8 Variation of torque at HI shaft with time (with TCSC)

5.5 Summary

This chapter presented the investigations of the subsynchronous resonance damping using TCSC under small disturbances. These investigations are conducted on the IEEE first benchmark model which consists of a large turbine-generator connecting to an infinite bus system through a series capacitor compensated transmission line.

The analysis was performed by modeling the individual systems (synchronous generator, electric network, and turbine-generator mechanical system) separately. The dynamic equations are linearized and combined in a single expression. These set of linearized equations were grouped and mathematically manipulated in order to obtain the overall system model in a state-space form.

It is observed that the TCSC also provides sufficient damping torque to the system to mitigate sub-synchronous phenomenon.

Chapter 6
CONCLUSIONS AND FUTURE SCOPE

6.1 Conclusions

Eigenvalue studies and time domain simulations conducted on the IEEE First Benchmark Models show the damping benefits on SSR of IMDU and TCSC. The major findings of the study are as follows.

1) The inclusion of the IMDU on the T-G shaft can eliminate torsional interaction type of SSR oscillations without the aid of any other controller.
2) The TCSC also damp SSR to a great extent. Besides damping SSR, it also works as to control active power flow. So TCSC is much more effective than IMDU.
3) In case of IMDU there is no need of any external controller so design difficulties reduces to a much low level as compared to TCSC where there need extra effort to design a suitable controller.
4) The IMDU can suppress SSR over the entire range of power transfer conditions and line compensation levels.
5) The IMDU and TCSC does not eliminate torque amplification; however, they reduces the torsional stresses on the shaft sections during large transients.
6) The IMDU is a small-size high power and low energy induction machine connected in mechanical system of Machine, whereas TCSC is connected along the network.
7) The HP turbine at the HP end of the shaft offers the best location for the IMDU for the FBM.
8) The IMDU does not affect the initial dynamic response of the T-G; therefore, it can be switched on only after a disturbance exciting torsional interaction is detected.
9) The IMDU does not affect the response of the generator to transient stability.
10) TCSC are already installed and working well whereas IMDU is a new concept to damp SSR.
11) The range of value of k (slope of torque speed characteristics) lies between 3 to 5 for successful damping of SSR by IMDU.
12) The whole system is need to be replaced with new one if we go for IMDU damping because of its mechanically connected to T-G shaft where In case of TCSC it can be installed anywhere along the line.

So overall we can say that SSR damping using IMDU is topic of great research. It has greatest advantage of being independent of any external controller but limit is also that it has to be mechanically connected to generator as compared to TCSC where it can be installed anywhere along the line and also has extra role of being able to control active power flow as well.

6.2 Future Scope

In this thesis we have discussed about damping SSR with the help of IMDU and TCSC using IEEE FBM. We can extend this thesis to include

1. We can include IEEE Second benchmark model for more realistic results.
2. We can design a suitable auxiliary controller for better control and operation of TCSC.

REFERENCES

[1] IEEE Subsynchronous ResonanceWorking Group, "Terms, definitions and symbols for subsynchronous oscillations," *IEEE Trans. Power App. Syst.*, vol. PAS-104, no. 6,pp. 1326–1334, Jun. 1985.

[2] O. Wasynczuk, "Damping shaft torsional oscillations using a dynamically controlled resistor bank," *IEEE Trans. Power App. Syst.*, vol. PAS-100, no. 7, pp. 3340–3349, Jul. 1981.

[3] E. Gustafson, A. Aberg, and K. J. Astrom, "Subsynchronous resonance. A controller for active damping," in *Proc. 4th IEEE Conf. Control Applications*, Sep. 1995, pp. 389–394.

[4] N. Kakimoto and A. Phongphanphanee, "Subsynchronous resonance damping Control of thyristor-controlled series capacitor," *IEEE Power Eng. Rev.*, vol. 22, no. 9, p. 63,Sep. 2002.

[5] H. Sugimoto, M. Goto, W. Kai, Y. Yokomizu, and T. Matsumura, "Comparative studies of subsynchronous resonance damping schemes," in *Proc. Int. Conf. Power System Technology*, Oct. 2002,vol. 3, pp. 1472–1476.

[6] M. R. Iravani and R. M. Mathur, "Damping subsynchronous oscillations in power systems using a static phase-shifter," *IEEE Trans. Power Syst.*, vol. 1, no. 2, pp. 76–82, May 1986.

[7] L.Wang and Y. Y. Hsu, "Damping of subsynchronous resonance using excitation controllers and static VAr compensations: A comparative study," *IEEE Trans. Energy Convers.*, vol. 3, no. 1, pp. 6–13, Mar. 1988.

[8] B. K. Perkins and M. R. Iravani, "Dynamic modeling of a TCSC with application to SSR analysis," *IEEE Trans. Power Syst.*, vol. 12, no. 4,pp. 1619–1625, Nov. 1997.

[9] X. Zhao and C. Chen, "Damping subsynchronous resonance using an improved NGH SSR damping scheme," in *Proc. IEEE Power Eng. Soc. Summer Meeting*, Jul. 1999, vol. 2, pp. 780–785.

[10] W. Li, L. Shin-Muh, and H. Ching-Lien, "Damping subsynchronous resonance Using superconducting magnetic energy storage unit," *IEEE Trans. Energy Convers.*, vol. 9, no. 4, pp. 770–777, Dec. 1994.

[11] A. H. M. A. Rahim, A. M. Mohammad, and M. R. Khan, "Control of subsynchronous resonant modes in a series compensated system through superconducting magnetic energy storage units," *IEEE Trans. Energy Convers.*, vol. 11, no. 1, pp. 175–180, Mar. 1996.

[12] O. Wasynczuk, "Damping subsynchronous resonance using energy storage," *IEEE Trans. Power App. Syst.*, vol. PAS-101, no. 4, pp. 905–914, Apr. 1982.

[13] S. K. Gupta, A. K. Gupta, and N. Kumar, "Damping subsynchronous resonance in power systems," *Proc. Inst. Elect. Eng., Gen., Transm.,Distrib.*, vol. 149, no. 6, pp. 679–688, Nov. 2002.

[14] K. Narendra, "Damping SSR in a series compensated power system," in *Proc. IEEE Power India Conf.*, 2006, p. 7.

[15] S. Purushothaman, "Eliminating Subsynchronous oscillations with an Induction Machine Damping Unit(IMDU)" IEEE Trans. On Power System, vol. 26, No. 1,Feb. 2011.

[16] IEEE Subsynchronous Resonance Task Force, "First benchmark model for Computer simulation of subsynchronous resonance," *IEEE Trans. Power App. Syst.*, vol. PAS-96, no. 5, pp. 1565–1572, Sep. 1977.

[17] D. Walker, C. Bowler, R. Jackson, and D. Hodges, "Results of subsynchronous resonance test at Mohave," *IEEE Transactions on Power Apparatus and Systems*, vol. 94, no. 5, pp. 1878–1889, 1975.

[18] K. R. Padiyar, Power System Dynamics stability and control, BS Publication, second Edition,2008.

[19] G. Pillai, A. Ghosh, and A. Joshi, "Torsional interaction studies on a power system compensated by SSSC and fixed capacitor," *IEEE Transactions on Power Delivery*, vol. 18, no. 3, pp. 988–993, 2003.

[20] A. A. Edris, "Subsynchronous resonance countermeasure using phase imbalance," *IEEE Transactions on Power Systems*, vol. 8, no. 4, pp. 1438–1447, 1993.

[21] P. Kundur, Power system stability and control, New York: McGraw-Hill, 1994.

[22] IEEE Task Force,"Current usage and suggested practices in power system stability Simulations for synchronous machines", IEEE Trans. On Energy Conversion, Vol. EC-1,No.1, 1986, pp. 77-93

[23] IEEE Subsynchronous Resonance Working Group, "Second benchmark model for computer simulation of subsynchronous resonance," IEEE Trans. Power App. Syst., vol. PAS-104, no. 5, pp. 1057–1066, May 1985.

[24] Paolo Mattavelli, Alexander M Stankovic and George C Verghese, .SSR Analysis with Dynamic Phasor Model of Thyristor Controlled Series Capacitor ., IEEE Transactions on Power Systems, Vol. 14, No. 1, pp. 200-208, February 1999.

[25] N. G. Hingorani, L. Gyugyi, Understanding FACTS: concepts and technology of flexible AC transmission systems, New York: IEEE Press, 2000.

[26] J. Butler and C. Concordia, “Analysis of series capacitor application problems,” *IEEE Transactions*, vol. 56, pp. 975–988, 1937.

[27] D. Walker, C. Bowler, R. Jackson, and D. Hodges, “Results of subsynchronous resonance test at Mohave,” *IEEE Transactions on Power Apparatus and Systems*, vol. 94, no. 5, pp. 1878–1889, 1975.

[28] J. Vithayathil, C. Taylor, M. Klinger, and W. Mittelstadt, “Case studies of conventional and novel methods of reactive power control on an ac transmission system,” ser. CIGRE paper, Paris, France, 1988, pp. 38 – 02.

APPENDIX A

Load Flow Program In MATLAB

To calculate the initial condition.

```
clc
P=0.7;
R=0;
phi0=acos(0.9);
Eb=1+j*0;
Xe=0.35;Xq=1.710;Xd=1.79;X1d=0.169;X1q=0.228;
%==================================================
Pt=P/cos(phi0);
Q=Pt*sin(phi0)
S=P+j*Q;
Ia0=S/Eb;
Vt0=Eb+(Ia0*(R+j*Xe));
theta0=angle(Vt0);
Eq0=Vt0+j*Xq*Ia0;
delta0=angle(Eq0);

Id0=-1*abs(Ia0)*sin(delta0-phi0)
Iq0=abs(Ia0)*cos(delta0-phi0)

Efd0=abs(Eq0)-(Xd-Xq)*Id0

E1q0=Efd0+(Xd-X1d)*Id0
E1d0=-(Xq-X1q)*Iq0

Vd0=-1*abs(Vt0)*sin(delta0-theta0)
Vq0=abs(Vt0)*cos(delta0-theta0)

sied0=(X1d*Id0)+E1q0
sieq0=(X1q*Iq0)-E1d0
```

APPENDIX B

SYSTEM DATA

B.1 Electrical Parameters

Table B-1. Network impedances, (in per unit, base: 892.4MVA, 500 kV)

Parameter	Positive Sequence	Zero Sequence
R_L	0.02	0.50
X_T	0.14	0.14
X_L	0.50	1.56
X_{sys}	0.06	0.06
X_C	0.35	0.35

Table B-2. Synchronous machine parameters, (in per unit, base: 892.4MVA, 26 kV)

Reactance	Value, p.u.	Time Constant	Value, *second*
x_d	1.790	T_{do}'	4.300
x_d'	0.169	T_{do}''	0.032
x_d''	0.135	T_{qo}'	0.850
x_q	1.710	T_{qo}''	0.050
x_q'	0.228		
x_q''	0.200		

B.2 Mechanical Parameters

Table B-3. Shaft inertia and spring constants

Mass	**Shaft**	**Inertia M** (Seconds)	**Spring constant *K*** (p.u./rad)
EXC		0.0342165	
	GEN-EXC		2.822
GEN		0.868495	
	LPB-GEN		70.858
LPB		0.884215	
	LPA-LPB		52.038
LPA		0.858670	
	IP-LPA		34.929
IP		0.155589	
	HP-IP		19.303
HP		0.092897	
	IMDU-HP		70.8
IMDU		0.034248645	